The Economic Cost of Locking down like China:

Evidence from City-to-City Truck Flows*

Jingjing Chen[1], Wei Chen[2], Ernest Liu[3], Jie Luo[4], and Zheng Song[5]

[1]*School of Economics and Management, Tsinghua University*
[2]*School of Economics, Zhejiang University*
[3]*Department of Economics, Princeton University*
[4]*School of International Trade and Economics, University of International Business and Economics*
[5]*Department of Economics, The Chinese University of Hong Kong*

November 12, 2024

Abstract

Containing the COVID-19 pandemic by non-pharmacological interventions is costly. Using high-frequency, city-to-city truck flow data, this paper estimates the economic cost of lockdown in China, a stringent yet effective policy prior to the Omicron surge. By comparing the truck flow change in the cities with and without lockdown, we find that a one-month full-scale lockdown causally reduces the truck flows connected to the locked down city in the month by 54%, implying a decline of the city's real income with the same proportion in a gravity model of city-to-city trade. We also structurally estimate the cost of lockdown in the gravity model, where the effects of lockdown can spill over to other cities through trade linkages. Imposing full-scale lockdown on the four largest cities in China (Beijing, Shanghai, Guangzhou, and Shenzhen) for one month would reduce the real national GDP by 8.7%, of which 8.5% is contributed by the spillover effects.

*We are grateful for comments by the editor, Daniel Sturm, and the two anonymous referees. We thank Ying Bai, Elisa Giannone (discussant), Wen-Tai Hsu, Steve Redding, and seminar participants at Tsinghua University and ABFER for helpful comments. We also thank Jin Han and Peikai Li for the excellent research assistance. Zheng Song acknowledges financial support from Hong Kong Research Grant Council and the Key Program of NSFC (Grant No. 71933001). Jie Luo acknowledges financial support from the Fundamental Research Funds for the Central Universities in UIBE (Grant No. CXTD14-04). The data and code that support the findings of this study are openly available at https://doi.org/10.3886/E210761. Corresponding author at Zheng Song, E-mail: zheng.michael.song@gmail.com.

1 Introduction

Many countries implemented non-pharmacological interventions such as stay-at-home mandate (lockdown) in the ongoing COVID-19 pandemic. The stringency and effectiveness of the interventions vary across countries. On the one hand, there is compelling empirical evidence that lockdown has a limited effect on the spread of coronavirus or death in Europe and North America.[1] On the other hand, lockdown appears to be more effective in flattening the curve of COVID-19 in the Asia-Pacific region, where the pandemic led to more aggressive policy responses before the emergence of Omicron.[2] China's zero-COVID policy was particularly effective. Hale et al. (2022a), for example, document that the first stay-at-home order was followed by a more than 90% decline in the number of confirmed new cases in China. The pattern was less dramatic in other Asia-Pacific countries and even reversed in the US, Canada and most European countries. It is hardly surprising that a communicable disease can be contained by sufficiently strict non-pharmacological interventions. The question is how much cost a country would have to pay for locking down like China.

Lockdown causes short-term losses of goods and services as well as various more persistent social costs. However, even the narrowly defined economic cost of a lockdown remains largely obscured to both the scientific community and policymakers. The main challenge is two-fold. First, it is hard to isolate the effect of policy intervention in a pandemic, in which other factors like fear-driven individual choices also contribute to economic losses (see, e.g., Goolsbee and Syverson, 2021). Moreover, since policy responds to the severity of the pandemic, endogeneity is an impediment to causal inference. Second, the effect of policy intervention, even if confined to a single locality, will spill over into all the other connected areas through economic linkages (see, e.g., Baqaee and Farhi, 2020; Bonadio et al., 2020). Such policy spillovers are hard to uncover by conventional locality-specific economic statistics.

Interestingly, China's draconian lockdowns themselves provide an ideal opportunity to tackle the identification issue. Since the epidemic broke out in Wuhan, the Chinese authority has developed a policy package that aims at zero local transmission of COVID cases. Lockdown plays a central role. A new COVID case immediately activates local lockdown, which may escalate to full-scale citywide lockdown within several days. The fact that most lockdowns were speedily implemented in response to even the smallest outbreak minimizes the endogeneity of policy responses. Moreover, the swift and stringent lockdowns are effective. Local outbreaks had all been very small until Omicron emerged. This bounds the effect of self-preventive measures by fear of infection.[3] But its success with less transmissible variants of COVID-19 already

[1] See, for example, Berry et al. (2021); Bendavid et al. (2021); Atkeson et al. (2020) and a dozen more empirical studies reviewed by Allen (2022).

[2] See, e.g., Ahn (2021) and Tang and Li (2021), for evidence from the Asia-Pacific region.

[3] The three most severe local outbreaks before Omicron came are Shijiazhuang, Yangzhou and Xi'an. The

makes the question highly valuable: How much cost do we have to pay to contain COVID by lockdown?

To deal with the second challenge, we employ a unique data set on monthly city-to-city truck flows. The data are from one of China's leading logistics service providers, which tracks real-time GPS information on 1.8 million (20% of China's) long-haul trucks in 2020.[4] The truck flow data has two advantages over the conventional economic statistics. First, the data is high frequency and can capture instantaneous truck flow changes, which can be one-to-one translated into real income changes in a gravity model of city-to-city trade. Second, the data capture not only city-specific economic activities but also city-to-city economic flows; the network nature of our data is central to our analysis. These features enable us to map out the real income change in response to lockdowns, from which we can further back out the spillover effect of a lockdown through the trade linkage.

We collect and compile a new data set on city-level lockdowns in China. The sample period starts from April 2020, when the Wuhan lockdown ended, to January 2022, before the Omicron surge. The cities experiencing citywide or main urban district lockdowns are classified as full-scale lockdowns, while the cities with some counties or districts locked down as partial lockdowns. We find that full-scale and partial lockdowns were imposed on 16 and 18 cities, with an average duration of 24 and 19 days, respectively. 32 out of the 34 cities were locked down only once.

Our empirical analysis starts with an event study approach. We provide evidence for parallel trends and against anticipatory effects. We then employ a two-way fixed effects regression that compares the truck flow between the cities of which at least one is in lockdown and the truck flow between the cities of which neither is in lockdown. A one-month full-scale lockdown reduces the truck flow connecting to the city in the month by 59%. The effect of a partial lockdown is 20%.

While all the COVID outbreaks after 2020 Q1 in our sample period were small, self-preventive measures driven by fear might still contribute significantly to the collapse of truck flow in full-scale lockdowns. Goolsbee and Syverson (2021) find the effect of shelter-in-place (S-I-P) order on consumer traffic to be small in the US. Moreover, the effect of fear appears to be strongly correlated with the number of local COVID deaths. To control for individual responses to the severity of local COVID outbreak, we add the number of COVID cases to the regression. The estimated effect of full-scale lockdown reduces marginally to 54%. If both

three cities were locked down in an average of 7 days after the first new case was found, with an average of only 111 COVID cases recorded (11.6 per million). However, the daily new cases, most of which were asymptomatic and detected in mandatory mass testing, are still an order of magnitude less than the peak in Hong Kong, where no lockdown or mass testing was implemented.

[4]Time-series aggregate statistics of the data have been used for descriptive analysis on China's economic responses to COVID-19 by both academics (e.g., Chen et al., 2021a) and market analysts (e.g., CICC, 2020).

consumer traffic and truck flow can measure local real income, our results would indicate that the full-scale lockdown in China inflicts much larger damage to the local economy than the S-I-P order in the US.

The reduced-form estimation, despite simple and highly transparent, is potentially flawed because it does not consider the spillovers of lockdown and their feedback through the intercity economic network. The high frequency city-to-city truck flow data allow us to structurally estimate the Armington model, in which a lockdown affects the between- and within-city cost of producing and selling goods, which in turn affect each city's production. Our estimation suggests that a full-scale lockdown increases the between- and within-city cost by 69% and 147%, respectively. Consistent with the results from the reduced-form approach, the effects of a partial lockdown are much smaller.

The trade linkages transmit the effects of lockdown to the other cities. The advantage of the structural approach is that we can estimate the aggregate effect of a lockdown and decompose it into the local and spillover effects.[5] For example, our model suggests that putting Shijiazhuang, a city with a population of 11 million, into full-scale lockdown for one month would reduce the real national income by 0.4%. Imposing one-month full-scale lockdown on a big city like Beijing would knock 2.5% off China's real income in the month. The effect of locking down a city on the real national income is related to the city's economic size and its position in the network. Using Shapley Value regression, we find that city-level GDP and eigenvector centrality contribute almost equally to both the aggregate effect and spillover effect of locking down a city. Finally, we find enormous economic costs of implementing full-scale lockdown at the national level. If the government puts all the 315 Chinese cities in our sample into full-scale lockdown for one month, the real GDP of these cities in the lockdown month would decline by 52%.

There is a fast-growing literature on the economic impacts of COVID-19 through trade linkages (see, for example, Maliszewska et al., 2020; Bonadio et al., 2020; Eppinger et al., 2020; and Hsu et al., 2020; among many others). Due to limited data on international trade after the outbreak of COVID-19, that literature, to the best of our knowledge, has to simulate economic losses caused by COVID-19. A unique feature of this paper is the use of the the bilateral truck flow data that measures actual trade flows between Chinese cities. We can estimate, rather than simulate, the effects of lockdown shock in a trade model.

It should also be noted that our analysis has a few obvious caveats. First of all, our city-to-city truck flow data do not disaggregate flows by industry. The monthly official statistics by city and industry are nonexistent in China. Therefore, we cannot distinguish the heterogeneous effects of lockdown across industries (e.g., Dingel and Neiman, 2020), nor can we study

[5]The spillover effects are entirely driven by the general equilibrium effect. In the model, we can decompose the percentage change of the real national income caused by locking down a city into the effect on the real income of the city itself (local effect) and the effect on the real income of the other cities (spillover effect).

the implications of the associated sectoral reallocation that have been extensively analyzed in the recent literature (e.g., Krueger et al., 2020; Gottlieb et al., 2022). Second, the same data limitation prevents us from analyzing the effect of lockdown transmitted through both input-output and trade linkages, an important channel studied in the recent COVID literature on international trade. The third caveat is that the contingency of lockdown might affect expectations and lead to intertemporal adjustments (e.g., Guerrieri et al., 2020) that are entirely absent in our study.

We contribute to the literature assessing the economic impact of COVID-19 and lockdown policies. Since the literature has been expanding rapidly, it is hard to give a comprehensive review. Many studies look into consumption expenditure change during the lockdown period in the first half of 2020 relative to the same period in the previous year. Cross-country comparison of the results provides some rough estimates of economic losses caused by lockdown outside China. As noted in Andersen et al. (2020), if we use Sweden as a counterfactual of no lockdown, where consumption expenditure fell by 25% between March 11 and April 5, most of the 27% consumption expenditure decline in Denmark between March 11 and May 3 would be attributed to the virus itself, rather than the mandate lockdown orders. This echoes the finding in Goolsbee and Syverson (2021) that individual responses account for most of the decline in consumer traffic in the US. The quarterly GDP data are also informative. Italy implemented relatively strict lockdown policies among European countries. The difference in the GDP change in 2020 Q2 between Sweden and Italy implies lockdown in Italy reduces its quarterly GDP by 5.7%. Allen (2022) also uses Sweden as a counterfactual to argue that the effect of Canadian lockdowns on GDP in 2020 Q2 is 5.1%. To the extent that truck flows are proportional to GDP, our estimates suggest that a one-month full-scale lockdown in all Chinese cities in our sample reduces GDP by 17.3% in the quarter.[6] The economic losses caused by Chinese lockdowns are three times as large as those caused by Italian and Canadian lockdowns.[7]

Our paper is also related to the research on the economic impact of COVID in China. Most papers focus on the first wave of the pandemic in the first quarter of 2020. While the first wave and the associated aggregate economic impact are larger by an order of magnitude,

[6] A one-month full-scale lockdown reduces monthly GDP by 52%. Under the assumption of uniform monthly GDP distribution within a quarter, this translates to a 17.3% decrease in quarterly GDP.

[7] The literature has also looked into employment and electricity consumption. See, for example, Montenovo et al. (2020), Forsythe et al. (2020), Adams-Prassl et al. (2020) and Buechler et al. (2022). There are other aspects of the economic consequences of COVID-19 and lockdown policies. Coibion et al. (2020) analysed how the timing of local lockdowns causally affects households' spending and macroeconomic expectations. Altig et al. (2020) constructs several indicators to measure the economic uncertainty in reaction to the pandemic and its economic fallout. Hensvik et al. (2021) explore real-time data on vacancy postings and job ad views on Sweden's largest online job board. Brodeur et al. (2021) use Google Trends data to show the effect of the pandemic and lockdown on mental health. The heterogeneous impacts of lockdowns are investigated by, e.g., Palomino et al. (2020), Bartik et al. (2020), and Chetty et al. (2020). Other studies on consumption and employment include, e.g., Diewert and Fox (2020), Alexander and Karger (2023), and Birinci et al. (2021).

the virus swept almost all cities and local policies responded to the severity of the epidemic, making the identification much harder. Fang et al. (2020), Chen et al. (2021) and Ai et al. (2022) employ the difference-in-differences (DiD) strategy to disentangle the effect of lockdown on mobility, consumption expenditure and electricity consumption, respectively, by comparing the lockdown and pre-lockdown periods in 2019 and 2020. He et al. (2020) and Pei et al. (2022) quantify the impact of lockdown on city's air pollution and year-on-year growth rate of exports by comparing locked down and non-locked down cities in 2020 Q1. Our identification is also based on the comparison between locked down and non-locked down cities. However, we explore a sample period with no major COVID-19 outbreak even in the locked down cities. This limits the endogenous individual and policy responses to severe outbreaks, which might differ between locked down and non-locked down cities when the virus swept across the country. The data set we compile on city-level lockdowns in China also complements the province-level indices constructed by Hale et al. (2022b).

Methodologically, we extend the first-order sufficient statistics in Kleinman et al. (2024) to obtain a closed-form formula that recovers productivity and trade cost shocks from over-time changes in trade flows. The first-order approach greatly reduces the computational cost of structural estimation. We also derive sufficient statistics that map from the shocks to welfare changes. Allen et al. (2020) derive the existence and uniqueness of equilibrium in trade and economic geography models as well as the first-order effect of trade cost shocks on equilibrium prices. We focus on how quantity, instead of price, responds to bilateral shocks. Unlike the standard Head and Ries (2001)'s method (see also Eaton et al., 2016; and Buera and Oberfield, 2020), which recovers the *levels* of trade costs from bilateral trade *expenditures* under the assumption that trade costs are symmetric, our sufficient statistics instead invert the over-time *changes* in the *quantity* of bilateral trade into *changes* in trade costs that fully rationalize the data.

Finally, our work also relates to the literature that jointly models the economic decisions and epidemics to quantify the economic costs and benefits of different policies (e.g., Eichenbaum et al., 2021; Krueger et al., 2020; Auray and Eyquem, 2020; Atkeson, 2020; Alvarez et al., 2020; Aum et al., 2021). The focus of our model is entirely on city-to-city trade that maps truck flows to real income. On the empirical side, we provide an estimate of economic cost associated with sufficiently strict lockdown that can swiftly contain the spread of COVID-19.

The paper is organized as follows. Section 2 summarizes several basic features of China's lockdown policy as well as the truck flow data. The reduced-form approach and its results are provided in Section 3. We present the model in Section 4. Section 5 shows the structural approach and its results. Section 6 reports the economic costs of lockdown in the structurally estimated model. Section 7 concludes.

2 Basic Facts

2.1 China's COVID Policy

The first COVID-19 outbreak in Wuhan prompted the Chinese government to implement draconian policies including locking down essentially all the cities in Hubei province, of which Wuhan is the capital city. The strict measures were effective. By April 2020, new COVID cases almost disappeared. After that, the Chinese authority developed and implemented a policy package that aims at zero local transmission of COVID cases, which is often referred to as zero-COVID policy. Notwithstanding sporadic local outbreaks, there was no nationwide outbreak before the emergence of the Omicron variant. The solid line in Figure 1 plots the number of monthly new confirmed cases in log units.[8] The average number of new confirmed cases since April 2020 is about two orders of magnitude smaller than that in the first quarter of 2020. As of the end of 2021, China's total COVID cases per million people are 73, among the lowest worldwide.[9]

China's zero-COVID policy is mainly based on non-pharmacological interventions. Some immediate policy responses, such as testing, contact tracing and quarantine, are commonly adopted elsewhere, though the reaction of the Chinese government is often perceived faster and better implemented than many other countries (Lazarus et al., 2020). Some preemptive measures are also tighter and more persistent. For example, strict border controls, together with at least two-week hotel quarantine for cross-border travelers, has been in place since the pandemic spread to other countries. Yet, the defining feature of China's zero-COVID policy is its determination to extinguish nascent outbreaks by draconian lockdown measures to even the slightest local outbreak. We summarize the guidelines for lockdown policy issued by the State Council according to an official explanatory document.[10]

Lockdown starts at community. The Chinese government classifies the communities recording positive but less than or equal to ten COVID cases in the past 14 days as "median-risk" zone. Those recording more than ten COVID cases are classified as "high-risk" zone. The median- and high-risk zones are "sealed" ("*fengkong*" in Chinese). All residents in the zones have to stay at home and be tested multiple times, and all vehicles, unless delivering necessities, are prohibited from entering the zones. According to the standards in Hale et al. (2020), median-

[8] We use the information released by local Health Commissions, collected by DingXiangYuan (https://ncov.dxy.cn/). Note that only locally transmitted cases with symptom are counted as new confirmed cases. At the national level, the asymptomatic cases that are tested positive but have never developed symptom account for 68% of total asymptomatic cases in our sample period, fewer than a fifth of the total confirmed cases. Many local governments do not report the asymptomatic cases.

[9] COVID cases can be underestimated for various reasons. Because our empirical analysis will exploit cross-route and over-time variation with route and time fixed effects, the results will not be affected by under-reporting of COVID cases at the aggregate level.

[10] We cannot find the original document issued by the State Council. The explanatory document we use is from Chengdu Health Commission and publicly available at https://www.sc.gov.cn/10462/10464/13722/2021/11/10/d0c69ea270c643578fa1fbc77e4a2272.shtml.

Figure 1: New COVID Cases and Total Truck Flow Change

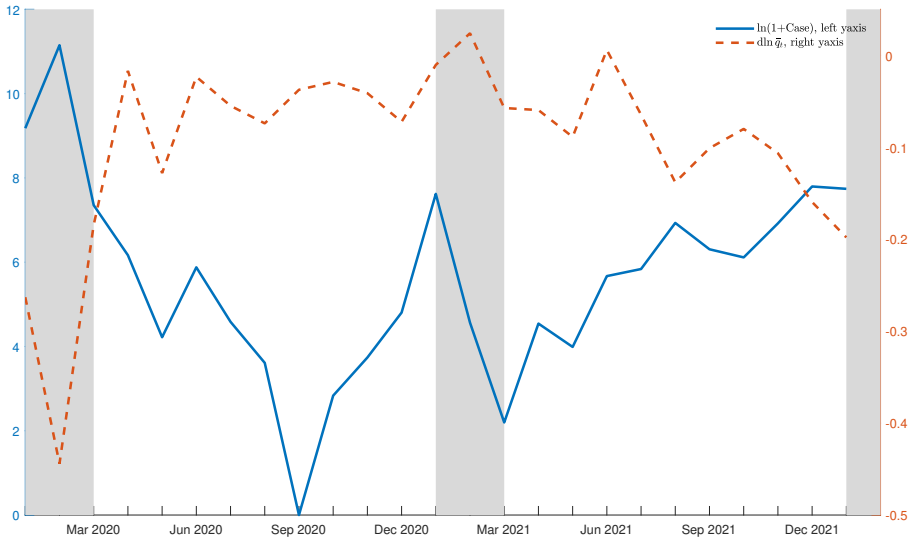

Note: The solid line is the log of new COVID cases in the month (left axis). The dashed line (right axis) is the aggregate detrended truck flow change, $\mathrm{d}\ln\bar{q}_t$, which is defined in the text. The grey shaded areas represent the first quarter.

and high-risk zones can be coded with the highest scale in all the categories for closures and containment. The restrictions, supposedly enforced by 24-hour patrols, are much stricter than those in Europe and North America. For instance, "staying at home" in China literally means no single step out of your door during the entire lockdown period, while the British version of "stay-at-home" order allows shopping for basic necessities and one form of out-door exercise a day.

The county or district to which the locked down community belongs is also affected, even if no cases are recorded elsewhere in the area. Lockdown-like restrictions are imposed on the "controlled" ("*guankong*") zones – i.e., the communities which the COVID infected individuals travelled to within two days before they were confirmed and are likely to cause local transmission. In particular, the residents in the controlled zones cannot leave home except to purchase necessities every two or three days. The communities other than the "sealed" and "controlled" zones in the county or district are all "guarded" ("*fangfan*"). The residents cannot leave the guarded zone unless for necessary trips such as seeking medical treatment, which requires a certificate of negative test result within 48 hours. Other measures for the guarded zones include encouraging working from home, restricting group gathering, closing indoor public places, and limiting restaurant dining.

We refer to lockdowns imposed on communities in a city as minimum lockdowns. The measures will escalate into locking down counties or districts in the city, referred to as partial

lockdowns, if there is evidence of community transmission. In the worst scenario, referred to as full-scale lockdown, the entire city or main urban district is locked down. The conditions for escalation are mainly determined by the severity of COVID outbreak. Dr. Fu Gao, the head of China's CDC, provides an example of Shijiazhuang in an article for which he is the corresponding author (Chen et al., 2021b).[11] There are exceptions. For instance, Langfang was locked down alongside Shijiazhuang in January 2021. However, the decision for Langfang is perhaps based more on its proximity to Beijing (64 km) than on the severity of the outbreak (only one case recorded).

COVID policies adapt to the evolving transmissibility and lethality of the virus. The outbreak of Omicron forced governments in many countries to adjust their policy interventions. Several Chinese officials have soften the language when describing lockdowns in their campaign slogans, from "zero COVID" to "dynamic clearance". Yet, there had not been any measurable relaxation in China's lockdown policies during the time frame of this study. The average stringency index in Hale et al. (2022b) in the second half of 2021 is actually slightly higher than that in the first half. Therefore, we simply assume the stringency of lockdown to be time-invariant.

2.2 Measuring Lockdowns

To accurately measure the timing and duration of lockdowns, we collect and compile a novel data set of Chinese lockdowns. Fang et al. (2020) and He et al. (2020) identify lockdown for each Chinese city in 2020 Q1. However, no systematic measures of city-level lockdowns are available after the first quarter of 2020, and in particular the data are not published by China's official statistics.[12] To fill the blank, we compile a monthly city-level lockdown index to distinguish the scale of lockdown. This subsection describes the collection methodology and presents some summary statistics.

We start with full-scale lockdowns, where the entire city or main urban district is locked down. A well-known example is that Wuhan, where the COVID epidemic first broke out, locked down the entire city with 11 million people for more than two months. The lockdown measures that can be found in government announcements include suspension of all traffic, closed-off management for all residential buildings and no leaving allowed from the city (see, e.g., Fang et al., 2020; and Pei et al., 2022). We use web scraping to compile a new data set on full-scale lockdowns between April 2020 and January 2022. The first step is to manually

[11] Shijiazhuang, the capital city of Hebei province, recorded the first case on January 2, 2021. The first round of mass testing for the city, which was conducted from 6 to 9 January, detected 354 cases. The whole city was locked down on January 7 according to news reports.

[12] China's CDC frequently updates the list of median- and high-risk zones at the community level, according to the number of new locally transmitted COVID cases. However, there are few economic data available at the same granular level. Hale et al. (2022b) create a composite index for China's COVID policy responses at the provincial level.

collect local government announcements for the three most well-known lockdowns after 2020 Q1: Shijiazhuang, Yangzhou and Xi'an. While the announcements are all about lockdown, local governments seldom used the word of *fengcheng*, meaning "locking down the city" in Chinese. Instead, our reading detects three keywords that frequently appear in the official announcements: (1) closed-off management in all areas; (2) traffic controls on all roads; (3) public transport out of service. We then scrape the first 50 results by searching year, month, city name and the three keywords on Baidu, where the year, month and city refer to the month in the year when the city recorded new COVID cases. The scraped web pages are manually processed through two more steps. The first is to drop the irrelevant web pages, including those with inconsistent timing and location and those on traffic controls caused by non-COVID considerations (e.g., extreme weather conditions). The second is to select official announcements on lockdown in the remaining web pages. This procedure identifies 16 cities on which full-scale lockdown was imposed once after 2020 Q1. No cities experienced the most draconian lockdown more than once. The average duration of full-scale lockdowns is 24 days.

A less draconian response is to lock down a county or district in a city (e.g., partial lockdown). We replace city name in the above procedure with county/district name and repeat the procedure for all the counties and districts in the city. We find 22 partial lockdowns in 18 cities. Two cities experienced partial lockdown more than once. The average duration of partial lockdowns is 19 days.

The starting date of each full-scale or partial lockdown can be extracted from government announcements. The lockdowns are on average imposed 3 days after recording the first new case. The end of lockdown is not always openly announced. We can find the ending date for 32 out of all the 38 full-scale or partial lockdowns. For the 32 lockdowns with ending dates, the lockdowns are on average lifted 7 days before the "clearance" day – i.e., the first day when no new case is recorded over the past 14 consecutive days. For the remaining 6 lockdowns, we assume they all end 7 days before the "clearance" day.

Locking down communities (i.e., minimum lockdown) is the mildest response. According to the mandate of the State Council, minimum lockdown should be immediately implemented in the cities recording new cases. The periods in which a city records positive new COVID cases but has no partial or full-scale lockdown are regarded as minimum lockdown periods.[13]

Table 1 summarizes our findings. The appendix provides the full list of the 34 cities on which full-scale or partial lockdown were imposed. Not surprisingly, the scale of lockdown relates to the severity of the COVID outbreak. The average number of new cases per million people is 74.9, 24 and 6.2 in the cities with full-scale, partial and minimum lockdown, respectively.

[13]Since it is hard to measure the actual duration of a minimum lockdown, which might vary across regions and over time, we assume that the Chinese government uniformly locks down all the communities with new COVID cases in the past two weeks.

Table 1: Lockdowns after Q1 2020

Panel A: Citywide lockdowns after Q1 2020		
Number of city	Average city COVID cases	$\mathrm{d}\ln\bar{q}_t^h$
16	329 (74.9)	-0.48
Panel B: Partial lockdowns after Q1 2020		
Number of city	Average city COVID cases	$\mathrm{d}\ln\bar{q}_t^l$
18	108 (24.0)	-0.21
Panel C: Other community lockdowns after Q1 2020		
Number of city	Average city COVID cases	$\mathrm{d}\ln\bar{q}_t^m$
111	38 (6.2)	-0.03

Note: Average COVID cases are the new COVID cases in the lockdown period. The number in parentheses is the ratio of new COVID cases to the city population (per million). $\mathrm{d}\ln\bar{q}_t^k$ is the weighted average of the truck flow changes for the city pairs with $D_{ni,t}^k = 1$ relative to that for those with $D_{ni,t}^k = 0\ \forall k$. $k \in \{h, l, m\}$ stands for full-scale lockdown ($k = h$), partial lockdown ($k = l$) and minimum lockdown ($k = m$), respectively. See the text for more detailed definition.

2.3 Truck Flows

The city-to-city truck flow data comes from real-time truck GPS records of 1.8 million trucks operating in 336 out of 342 prefecture-level cities.[14] Specifically, the truck flow data measures the number of round-trip trucks that depart from a city identified as the place of loading and arrive at another city identified as the place of discharge. The city-to-city truck flow is symmetric by construction. Because trucking is the primary mode of domestic freight transport in China, truck flows are highly correlated with economic activities.[15] Figure A8 in the appendix shows that cross-sectionally city-level truck outflows correlate strongly to city-level GDP in 2019 (correlation 0.9) and also to night light intensity (correlation 0.86). The truck flow data does not contain information about freight.

This paper employs the truck flow data covering 315 cities from January 2019 to January 2022.[16] The logistics service provider does not monitor within-city truck flows. Truck flows are regularly updated on 60% of all the $315 \times 314/2 = 49,455$ between-city pairs. The city pairs with truck flow data are closer to each other and richer than those without.[17] To control for the effects of the growth trend of the economy and the expansion of the logistics service provider,

[14] See Alder et al. (2023) for a detailed description of the real-time GPS data.

[15] The Highway accounts for 73% of the total freight in China in 2019 by official statistics.

[16] We exclude cities in Tibet and Xinjiang, as these two regions have much fewer trade linkages to the rest of China.

[17] The difference is 35% less and 55% more in the between-city distance and total GDP, respectively.

we filter out the route-specific trend component in the time series of log truck flow.[18] Denote by $\ln q_{ni,t}$ the detrended log truck flow from city i to n at period t. To control for the seasonal effects, we take difference of the detrended log truck flow between the current period and the same period in 2019. The difference is referred to as the log change in truck flows and denoted by $\mathrm{d}\ln q_{ni,t}$. The aggregate truck flow change is measured by $\mathrm{d}\ln \bar{q}_t \equiv \sum_{ni} \omega_{ni} \mathrm{d}\ln q_{ni,t}$, where ω_{ni} is the weight measured by the city-pair's total truck flows in 2019.

Figure 1 shows that, in the time series, the aggregate truck flow change correlates negatively to new COVID cases (correlation -0.69). The negative correlation remains significant (correlation -0.42 with p-value 0.09) after removing data from the first quarter, a time window that contains the Chinese New Year (January 25 in 2020, February 12 in 2021 and February 1 in 2022), a major festival during which economic activities, COVID policies, and the outbreaks themselves may operate differently from the rest of the year.

To link city-level lockdown measures to the city-to-city truck flows, we construct city-pair lockdown dummies, $D^k_{ni,t}$, where $k \in \{h, l, m\}$ stands for full-scale ($k = h$), partial ($k = l$) and minimum lockdown ($k = m$), respectively. For $n \neq i$, $D^h_{ni,t}$ is a city-pair dummy that equals one if at least one of the cities has a full-scale lockdown in the period. Similarly, $D^l_{ni,t}$ equals one if at least one city has partial lockdown and no full-scale lockdown is imposed on any of the cities in the period. Likewise, $D^m_{ni,t}$ is the dummy variable for minimium lockdown, which equals one if any city in the pair records new COVID cases and none of the cities have full-scale or partial lockdown. For $n = i$, $D^h_{ii,t}$, $D^l_{ii,t}$ or $D^m_{ii,t}$ becomes a city dummy, which equals one if the city experiences full-scale, partial and minimum lockdown, respectively.

The decline of truck flows in the lockdowns is evident. Denote by $\mathrm{d}\ln \bar{q}^k_t$ the weighted average truck flow change for the city pairs with $D^k_{ni,t} = 1$ relative to that for $D^k_{ni,t} = 0\ \forall k$. Table 1 shows that $\mathrm{d}\ln \bar{q}^k_t$ for $k = h$ (full-scale lockdown) declined by 0.48 log points. The decline is 0.21 and 0.03 for $k = l$ and $k = m$ (partial and minimum lockdown), respectively.

In what follows, we will treat minimum lockdowns as no lockdown. This is based on the observations that the number of COVID cases and the disruption of truck flows are both small in minimum lockdowns. Section 3.1 will check the robustness of our results by estimating separately the effect of minimum lockdowns.

2.4 Normal and Lockdown Periods

Let $D_{ni,t} = D^h_{ni,t} + D^l_{ni,t} > 0$ be the lockdown dummy that equals one if at least one city has full-scale or partial lockdown at period t. We define a period $[N_0, N_1]$ as "normal" if there are no lockdowns in the broader time window from 2 months before to 2 months after the period – i.e., $D_{ni,t} = 0\ \forall t \in [N_0 - 2, N_1 + 2]$. We define $[T_0, T_1]$ as a "lockdown" period if there are lockdowns

[18] We use linear detrending. Using HP filter gives essentially the same results.

during $[T_0, T_1]$, but no lockdowns in the 4 months prior to T_0 and 4 months after T_1. We work with the sample that consists of all the lockdown periods, extended by 2 months forward and backward, and all the normal periods. This drops about 1.5% city-pair-month observations. As will be shown in the event study below, the restriction guarantees that there are no overlaps of lead-lag effects in the sample. Our sample has 2068 city-pair-month lockdowns. We do not distinguish the city pairs with one or both cities locked down since only 28 observations have both cities locked down.

3 Reduced-Form Approach

We first estimate the effect of lockdown on the directly observable city-to-city truck flows. We adopt a two-way fixed effect regression to estimate the effect of lockdown on $\mathrm{d}\ln q_{ni,t}$, for $n \neq i$.

$$\mathrm{d}\ln q_{ni,t} = \sum_{k\in\{h,l\}} \alpha^k D^k_{ni,t} + \delta_{ni} + \nu_t + \eta_{ni} t + \epsilon_{ni,t}, \tag{1}$$

where we control city-pair fixed effect, δ_{ni}, time fixed effect, ν_t, and city-pair-specific time trend, $\eta_{ni}t$. $\epsilon_{ni,t}$ is an error term, which has zero mean and can be serially correlated. Since $q_{ni,t} = q_{in,t}$, the regression does not distinguish between exporter and importer. Each observation is a city pair and always weighted by ω_{ni} (the city pair's total truck flows in 2019) to reduce the influence of outliers and measurement errors.

Equation (1) estimates the effect of type-k lockdown, α^k, by comparing the cities with type-k lockdown and those without lockdown in the same month. Identifying α^k requires two key assumptions. First, the average truck flows with and without lockdown would have followed parallel trends in the absence of lockdown. Second, lockdown has no causal effect prior to its implementation (no anticipatory effect). Both assumptions would be satisfied if lockdown is solely activated by random local COVID outbreaks.[19] Moreover, the parallel trends would still hold if the selection bias remains the same between the periods with and without lockdown. This can be checked by comparing trends of truck flows in the pre-lockdown period, which will be examined in Section 3.1.

Different from the canonical DiD specification, (1) has staggered treatments (lockdowns). In addition, they are not an absorbing state. The implications of staggered and non-absorbing treatments have been studied in the recent literature (see de Chaisemartin and D'Haultfœuille, 2020). We also need homogeneous treatment effects (i.e., constant β^k across routes and over time) for the OLS estimator to be unbiased. The recent literature addresses some limitations of the OLS estimator with staggered treatment and heterogeneous effects. We adopt a new

[19]The decision of lockdown may be affected by other factors. However, we do not find any correlation between the lockdown and the city's economic or population size (see Figure A9 in the appendix).

method and find the results to be very robust. The details are provided in Section A.2.

We can allow $n = i$ in (1) by inferring $\mathrm{d}\ln q_{ii,t}$ from (11), which assumes within-city truck flow to be a weighted average of between-city truck flow changes. However, by construction, the unweighted OLS estimate of the coefficient of $D^k_{ii,t}$ will be identical to that of $D^k_{ni,t}$ for $n \neq i$. While the reduced-form regression cannot distinguish the within- and between-city effects, they can be separately estimated in the structural approach.

Because lockdowns took place at the city-month level, another key assumption underlying our approach is that lockdowns are uncorrelated with other city-month level shocks that may affect city-to-city trade. We believe this is a good assumption in our context because (1) we use high-frequency (monthly) data; (2) lockdowns were speedily implemented in response to even the smallest outbreaks, which occurred plausibly exogenously; (3) actual outbreaks in our sample period were very small and unlikely to affect economic decisions except through the lockdowns. For these reasons, our baseline reduced-form specification deviates from that of a typical gravity regression in that we omit importer- and exporter-time fixed effects and include only the city-pair fixed effects and time fixed effects. Nevertheless, we will conduct several robustness checks in Section 3.2 on the validity of this assumption and the sensitivity of our results relaxing the assumption.

3.1 Results

Before estimating the model, we first check our identification assumptions by generalizing (1) to an event-study approach.

$$\mathrm{d}\ln q_{ni,t} = \sum_{k\in\{h,l\}} \left(\sum_{j=1}^{\bar{J}} \alpha^k_{-j} PRE^{k,j}_{ni,t} + \alpha^k_0 D^k_{ni,t} + \sum_{j=1}^{\bar{J}} \alpha^k_j POST^{k,j}_{ni,t} \right) + \delta_{ni} + \nu_t + \eta_{ni} t + \epsilon_{ni,t}. \quad (2)$$

Here, $PRE^{k,j}_{ni,t}$ is a dummy that equals 1 if t is j months before the beginning of the next type-k lockdown. Analogously, $POST^{k,j}_{ni,t}$ is a dummy that equals 1 if t is j months after the end of the previous type-k lockdown.

The estimated α^k_0 will capture the difference between truck flows in type-k lockdowns and those in normal periods. The estimated α^k_{-j} or α^k_j will capture the difference between truck flows in j months prior to or after type-k lockdowns and those in normal periods, respectively. We use the leads to verify the presence of pre-trends. The lags, if statistically significant, would suggest some persistent effects after the lockdown ends. $\underline{J}$ is set to 2 so that there are no lead-lag effects of other lockdowns in the 2 months prior to or after the lockdown in our sample.[20]

[20] Recall that we only keep the lockdowns that are at least four months away from the other lockdowns in the sample.

The results are reported in Figure 2. There is no evidence for pre-trends since the estimated α^k_{-j} are statistically insignificant. The estimates of α^k_0 are significant and quantitatively sizable. Imposing full-scale lockdown on city i will reduce the truck flows connected to the city by 0.41 log points. The effect of a partial lockdown is 0.10 log points. The estimates of α^k_1 and α^k_2 become insignificant and much smaller than that of α^k_0. These estimates suggest that the lockdown has no persistent effect on truck flows. We cluster standard errors at the city-pair level. Similar results can be found in Figure A10 if we cluster standard errors at both city n and i (Cameron et al., 2011).

Figure 2: Event Study

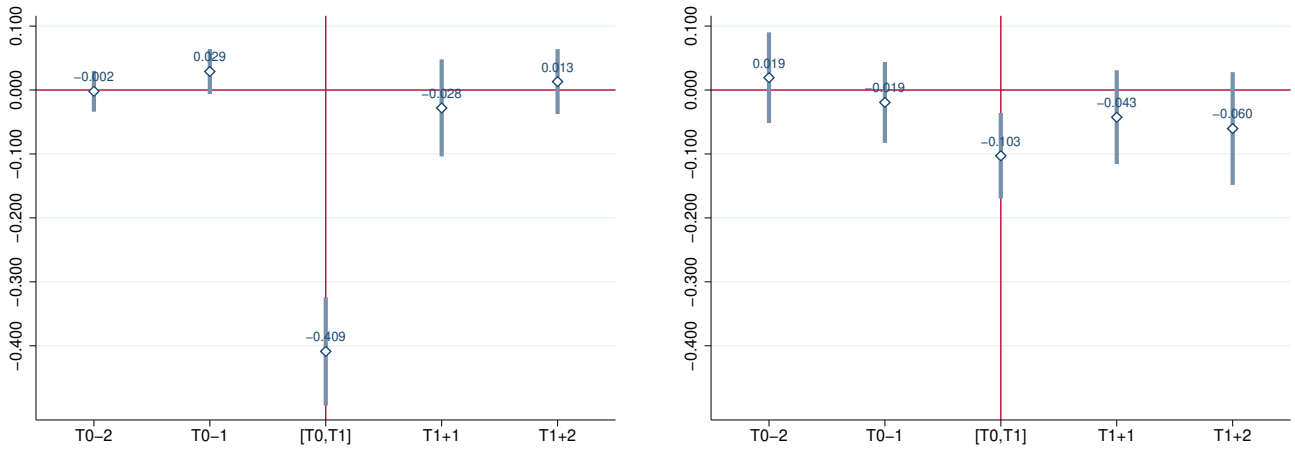

(a) Full-scale lockdown

(b) Partial lockdown

Note: The figure plots the estimated α^h_j (left panel) and α^l_j (right panel) in (2), together with their 95% confidence intervals. Each observation is weighted by ω_{ni}, the city-pair's total truck flows in 2019.

We then run the regression (1). The results are reported in the first column of Table 2. Not surprisingly, the estimate of α^k is very close to α^k_0 in the event study.

We have been treating cities with minimum lockdown as part of the control group. We can check the validity of our assumption by adding the COVID dummy to the regression. The COVID dummy for a city pair will be equal to one if any city in the pair records new COVID cases and none of the cities have full-scale or partial lockdown. Since minimum lockdown is automatically activated by a new COVID case, the COVID dummy is also a dummy for minimum lockdown in the city pair ($D^m_{ni,t}$). The results are reported in the second column of Table 2. The effect of minimum lockdown is statistically significant but quantitatively small. It only reduces truck flows by 0.03 log points. Moreover, the estimated α^h and α^l remain robust after controlling for minimum lockdown. These results are reassuring. Ignoring minimum lockdown will not significantly bias the estimates on the effects of full-scale and partial lockdown.

Table 2: Effect of Lockdown on Truck Flow, Panel Regression

	(1)	(2)	(3)	(4)	(5)
	D^k_{ni}			$\hat{D}^k_{ni}$	
Full-scale lockdown	-0.4093	-0.4171	-0.3508	-0.8931	-0.7695
	(0.0415)	(0.0418)	(0.0377)	(0.0656)	(0.0668)
Partial lockdown	-0.0911	-0.0963	-0.0403	-0.2182	-0.1063
	(0.0257)	(0.0256)	(0.0268)	(0.0622)	(0.0659)
COVID dummy		-0.0271			
		(0.0064)			
$\ln(1 + \text{Case})$			-0.0228		-0.0204
			(0.0028)		(0.0025)
Time FE	YES	YES	YES	YES	YES
City pair FE	YES	YES	YES	YES	YES
City pair trend	YES	YES	YES	YES	YES
Observations	206325	206325	206325	206325	206325
R-squared	0.3360	0.3369	0.3391	0.3379	0.3403

Note: The first two rows report the effect of lockdown on truck flows. Standard errors are clustered at city pair and reported in parentheses. Each observation is weighted by ω_{ni}, the city-pair's total truck flows in 2019. In Columns (1) to (3), we use D^k_{ni} to measure lockdown, which is a dummy that equals one if city pair (n, i) has type-k lockdown. In Columns (4) and (5), we use $\hat{D}^k_{ni,t}$, which represents the proportion of days with type-k lockdown in the month with $D^k_{ni,t} = 1$. COVID Dummy equals one if the city pair has new COVID cases and none of the cities have full-scale or partial lockdown. "Case" refers to the number of new COVID cases in the city pair.

Equation (1) assumes that lockdown is the only channel through which the pandemic can affect truck flows. Equation (1) can be extended by allowing truck flows to be affected by individual choices. Specifically, we assume that a more severe COVID outbreak will intensify self-protective measures that suppress economic activities and truck flows.

$$\mathrm{d}\ln q_{ni,t} = \sum_k \alpha^k D^k_{ni,t} + F(s_{ni,t}) + \delta_{ni} + \nu_t + \eta_{ni} t + \epsilon_{ni,t}, \tag{3}$$

where F is an increasing function and $s_{ni,t}$ measures the severity of the pandemic in the city pair (n, i). We assume $F(s_{ni,t}) = b \ln(1 + \text{Case}_{ni,t})$, where "Case" is the number of new COVID cases in the city pair.[21] The third column of Table 2 shows that, conditional on lockdown

[21] The results are robust to adding high-order polynomials to $F(s_{ni,t})$. Only the linear term would be signifi-

status, a more severe COVID outbreak is indeed associated with a larger decline in truck flows.

Moreover, the estimated α^h and α^l drop by 14% and 56%, respectively, after controlling for $F(s_{ni,t})$. Our finding confirms that lockdown should not be the only reason for the disruption to economic activities in lockdown. To the extent that the number of COVID cases correlates to fear of infection and self-protective measures, individual choices may account for a significant part of the decline in truck flows. That being said, the estimated α^h remains quantitatively large. A full-scale lockdown reduces truck flows by 0.35 log points on average. In contrast, the effect of COVID severity has the maximum of 0.17 log points for Xi'an, which recorded 2052 cases between December 2021 and January 2022. The estimates of partial lockdown become statistically insignificant after controlling for the number of COVID cases. The effects of policy interventions and individual responses to the pandemic may be harder to separate in less stringent lockdown.

We have so far used monthly lockdown dummies to match the monthly truck flow data. The monthly dummies, albeit simple, do not reflect the length of lockdown in a month. The full-scale lockdown in Langfang lasts for only 5 days, while Yangzhou was under full-scale lockdown in the entire month of August 2021. The average number of days of full-scale and partial lockdown in the lockdown month (not the whole lockdown period) with $D^h_{ni,t} = 1$ and $D^l_{ni,t} = 1$ are 14 and 12, respectively. To provide a more accurate measure of lockdown, we construct a continuous variable, $\hat{D}^k_{ni,t} \in (0, 1]$, which represents the proportion of days with type-k lockdown in the month with $D^k_{ni,t} = 1$. The last two columns of Table 2 show that the estimated coefficient of $\hat{D}^k_{ni,t}$ more than doubles that of $D^k_{ni,t}$. Controlling for COVID cases reduces the effect of full-scale lockdown by 14%. Imposing full-scale lockdown on a city for a whole month would reduce truck flows connected to the city by 0.77 log points. A whole month partial lockdown would reduce the truck flows by 0.11 log points.

3.2 Robustness

City-Specific Time-Varying Shocks We assume lockdown to be uncorrelated with other city-specific time-varying shocks affecting bilateral trade flow. We try two different approaches to examine the validity of and the robustness of the results to the assumption. First, we estimate exporter- and importer-month fixed effects and then use event study to show how lockdown affects the estimated fixed effects. Second, we interact exporter and importer dummies with year or semi-year dummies to control for the city-specific characteristics that vary at lower frequency. We show the empirical specifications and results in Appendix A.3. The estimated effect of full-scale and partial lockdown on the exporter- and importer-month fixed effects is -0.37 and -0.10 log points, close to the estimated effect of -0.41 and -0.10 on truck flows in the

cant.

benchmark case. The estimates are also very robust to the exporter and importer dummies interacted with year or semi-year dummies.

City-Level Regression While our main treatment is city-month lockdowns, the unit of observation in our baseline regressions is city-pair-month, capturing the effect of city-month shocks on monthly city-to-city trade flows. A simpler approach is to perform the regression at the city-month level. In Appendix A.4, we show that this specification, which is easier to interpret, introduces some bias to our estimates. This is because truck flows occur at the bilateral level, and strictly speaking there are no cities that are "untreated": locking down one city should affect city-level truck flows of all the other cities, as long as these cities trade with the locked down city. Empirically, we find the bias to be small.

Violation of SUTVA City-pair regression can reduce the above bias in city-level regression. However, lockdown of treatment pairs may still have an impact on the truck flows of control pairs through spillover or general equilibrium effects, which violate the Stable Unit Treatment Value Assumption (SUTVA). This is exactly the reason why we will use the structural approach. In addition, we conduct three additional robustness checks to address this important concern.

We first excluded the control pairs which are more likely affected by lockdown of the treatment pairs. One option is to use a "cleaner" control group in which the cities do not neighbor any locked down cities in the treatment group (see, e.g., He et al., 2020). Another option is to exclude the cities to which the lockdown cities are their important trading partners. We classify city n as an important trade partner of city i by the bilateral truck flows exceeding 1% of city i's total truck flows in 2019. We can also control for lockdowns along the routes in the control group. The details are provided in Appendix A.5. Our results are all robust to these alternative control groups.

The second approach is to adopt the simple first-difference estimation in Hanna et al. (2017). We select the routes that experienced lockdown at least once and estimate the effect of lockdown for each of the routes. This route-specific regression keeps the treatment and control groups in different periods. Therefore, lockdown does not affect the control group. Appendix A.5 shows the empirical specification and the distribution of the estimates across the routes. The average effect, weighted by the corresponding route's total truck flows in 2019, is -0.38 and -0.15 log points for full-scale and partial lockdown, respectively. They are, again, close to our main estimates.

Lastly, the reduced-form approach does not consider substitution of trade between the city that is under lockdown and the other cities that are not, which, again, violates SUTVA. While this issue will be taken care of by the structural approach, we can still employ the same reduced-form approach to check the magnitude of the bias. Specifically, we construct a city-level variable

that measures the change in total truck flows to the city's neighbors but excludes the change in truck flows from the city. If a city's trading partners can easily switch to another city, locking down the city should lead to an increase in truck flows to its neighbors. However, the effect appears to be small and insignificant. The details are provided in Appendix A.5.

City-to-City Population Flows Fang et al. (2020) estimate the effects of the first-wave lockdowns on population flows. Using the same data source from Baidu, we construct a sample of weekly city-to-city population flows that covers the Chinese new year period in 2021 and 2022 (up to January 31, 2022). The sample covers 8 out of 16 full-scale lockdowns and 10 out of 22 partial lockdowns in Table 1. We then apply the same event study approach to the change in weekly city-pair population flows.

Appendix A.6 reports the findings. They are qualitatively similar, though the estimated effects on population flows are larger. We are cautious about mapping changes in population flows into welfare effects. The main reason is that while goods trade must necessarily involve the physical mobility of goods from one location to another, cross-location worker flows can substitute from physical commutes into remote work, as documented by the recent literature focusing on remote work in the US (e.g., Barrero et al., 2021).[22]

4 Model

The reduced-form approach estimates the local effect of lockdown. To explore the spillover effect, we employ the standard Armington (1969) model of trade. We derive linear sufficient statistics that map changes in bilateral trade flows to changes in trade costs and real income. As is well-known in the trade literature (e.g., Arkolakis et al., 2012), the Armington model is isomorphic to the model in Eaton and Kortum (2002). Our results extend those in Kleinman et al. (2024), which derive linear sufficient statistics of productivity changes on real income. The first-order approach greatly reduces the computational cost of structurally estimating the cost of lockdown. We will perform policy counterfactuals based on our sufficient statistics and the recovered trade costs.[23]

Each city $n \in \{1, ..., N\}$ in China is modeled as an open and perfectly competitive economy endowed with a representative consumer who supplies ℓ_n units of labor inelastically to produce a city-specific goods with productivity a_n, or the production function $Q_n = a_n l_n$. Given wage

[22]By selection, workers are ex-ante less likely to commute across cities for jobs that require workers to be in close proximity; these jobs are thus less likely to be disrupted by the lockdowns. Hence, it is questionable how to infer about the welfare impact of lockdowns from the reduction in population flows.

[23]Although we choose the Armington formulation for simplicity, our results hold for any international trade model with a CES import demand system.

rate w_n, unit cost of producing goods in city n is

$$c_n = w_n / a_n. \tag{4}$$

Each consumer has a taste for variety, with utility function

$$\boldsymbol{u}_n = \left(\sum_{i=1}^{N} Q_{ni}^{\frac{\theta}{\theta+1}} \right)^{\frac{\theta+1}{\theta}}, \tag{5}$$

where Q_{ni} is the trade flows of goods i consumed in city n in quantity, and $\theta+1$ is the elasticity of substitution across goods. The terms "welfare", "real income", and "utility" are often used interchangeably in the literature. To avoid confusion, we will refer to $\boldsymbol{u}_n$ as "real income".

Cities trade with one another subject to iceberg-type proportional trade cost τ_{ni} for sending goods produced in i ("goods i" in short) to city n. The model predicts a gravity relationship for city-to-city bilateral trade flows:

$$\underbrace{Q_{ni} w_i \tau_{ni} / a_i}_{\substack{\text{city } n\text{'s expenditure} \\ \text{on goods } i}} = \underbrace{(w_n \ell_n + \bar{d}_n)}_{\substack{\text{city } n\text{'s} \\ \text{total expenditure}}} S_{ni}, \qquad S_{ni} \equiv \frac{(w_i \tau_{ni} / a_i)^{-\theta}}{\sum_{k=1}^{N} (w_k \tau_{nk} / a_k)^{-\theta}}, \tag{6}$$

where w_i is the cost of labor (wage rate) in city i; $w_i \tau_{ni} / a_i$ is the price of goods from i to n (p_{ni}); S_{ni} is the expenditure share of consumer n on goods i. An equilibrium is the set of quantities and wage rate $\{Q_{ni}, w_i\}_{i,n=1}^{N}$ that satisfies the expenditure share relationship in (6),[24] which states that the total income of city i is equal to the sum of expenditure on goods i by all other cities:

$$w_i \ell_i = \sum_{n=1}^{N} (w_n \ell_n + \bar{d}_n) S_{ni}, \tag{7}$$

where we choose the normalization that $\sum_i w_i \ell_i = 1$, and $\bar{d}_n$ is trade deficit, which is exogenously given in our model.[25]

Our model abstracts away from nontradable sectors, since our data do not distinguish truck flows by industry.[26] Our model also abstracts away from labor mobility, because inter-city migration is limited in the short run.

We use the system of equations (5), (6), and (7) to derive sufficient statistics that connect trade cost and productivity changes, trade flow changes as well as welfare changes, extending

[24] Market clearing holds by Walras law, (6) and (7).

[25] We assume the trade with the rest of the world does not change with the domestic shocks.

[26] The main findings are robust in a more general model with nontradable sectors under the assumption that city-level shocks apply equally to tradable and nontradable sectors.

the results in Kleinman et al. (2024).

Because a productivity change in city i is isomorphic to a uniform change in the shipping cost from i to all of its trading partners (including city i itself), we define $\mathrm{d}\ln z_{ni} \equiv \mathrm{d}\ln \tau_{ni} - \mathrm{d}\ln a_i$ as the composite change in trade cost and productivity in the route at which labor in city i produces goods consumed by city n.

We stack bilateral trade flow quantities Q_{ni}, expenditure shares S_{ni}, and composite cost z_{ni} into $N \times N$ matrices $\boldsymbol{Q}$, $\boldsymbol{S}$, and $\boldsymbol{Z}$, respectively. For notational ease, we further let $\boldsymbol{\mathcal{Q}}_{N^2\times 1}$ and $\boldsymbol{\mathcal{Z}}_{N^2\times 1}$ be the vector form of $\boldsymbol{Q}$ and $\boldsymbol{Z}$, respectively.

Proposition 1 *Starting from an equilibrium with expenditure share $\boldsymbol{S}$,*

(1). There is a one-to-one linear mapping from the composite cost shocks vector to the changes in bilateral trade flow quantities vector:

$$\mathrm{d}\ln \boldsymbol{\mathcal{Q}} = \boldsymbol{G}\,\mathrm{d}\ln \boldsymbol{\mathcal{Z}} \tag{8}$$

where $\boldsymbol{G}$ is an $N^2 \times N^2$ matrix that depends only on the trade elasticity θ, the expenditure share matrix $\boldsymbol{S}$.

(2). The real income change in city n:

$$\mathrm{d}\ln \boldsymbol{u}_n = \sum_{i=1}^{N} S_{ni}\,\mathrm{d}\ln Q_{ni}.$$

We leave the proof to the appendix. Intuitively, when the composite cost from i to n increases due to lockdowns ($\mathrm{d}\ln z_{ni}$), city n lowers its demand for goods i and raises demand for other goods. This partial equilibrium substitution effect lowers the income in city i and its production cost, thereby causing further rounds of substitution, through which the effect of $\mathrm{d}\ln z_{ni}$ affects prices, consumption, and real income in other cities $k \notin \{n, i\}$. The full, general equilibrium effect of composite cost shocks sums across all rounds of propagation and is disciplined by our trade model. The matrix $\boldsymbol{G}$ in Proposition 1 forms the linear sufficient statistics for these general equilibrium effects of COVID shocks. In subsequent sections, we use Proposition 1 to estimate the economic impact of lockdown policy and perform counterfactual analysis.

Under the assumptions that the composition of goods in trucks and the proportion of road transport in the total city-to-city freight do not change over time, the truck flow change is identical to the trade quantity change – i.e., $\mathrm{d}\ln Q_{ni,t} = \mathrm{d}\ln q_{ni,t}$. Then, the second part of Proposition 1 implies that the weighted average truck flow change on the routes to a city can be interpreted as the city's real income change. Moreover, as will be shown below, our linear

sufficient statistics allow a closed-form solution to the structurally estimated lockdown shocks, which greatly reduces computational costs of solving a large system of equations.[27]

Relation of Proposition 1 to the Literature Proposition 1 shows that in the Armington model, by observing changes in the full matrix of bilateral trade flow quantities ($\mathrm{d}\ln q_{ni}$), one can recover, to first-order, the full matrix of shocks to the composite bilateral trade costs and productivities ($\mathrm{d}\ln(\tau_{ni}/a_i)$) that would rationalize the trade flow changes. This inversion requires observing the initial bilateral expenditure shares and knowing the trade elasticity. The second part of the result then maps the quantity changes to welfare effects. These results are especially applicable in our setting: we observe changes in trade flows due to COVID lockdowns, and we use Proposition 1 to recover the implied bilateral shocks and study the local and spillover welfare impact of these shocks.

Proposition 1 is related to but, to our knowledge, different from several known results in the literature. Arkolakis et al. (2012) provide sufficient statistic for the counterfactual change in domestic welfare following a foreign shock. Our result instead provides an invertible mapping between bilateral shocks and bilateral trade flows for the entire economy, not just welfare changes in a single location. Allen et al. (2020) derive the first-order general equilibrium response of prices to trade cost shocks; Proposition 1 instead provides how quantities respond.[28] Kleinman et al. (2024) provide sufficient statistics of how equilibrium nominal and real income respond to trade cost shocks but also do not concern trade flow quantities.

5 Structural Approaches

A key advantage of the reduced-form approach is the simplicity of the event-study setting that enables us to estimate the effect of a lockdown in city i on truck flows involving city i. An important limitation of the approach is that are unable to estimate the general equilibrium spillover effects on truck flows along routes not involving cities under lockdowns.

We now use the model to estimate the general equilibrium and distributional effects of lockdowns. Conceptually, we structurally estimate the effect of lockdowns in two steps. First, we use the observed year-on-year trade flow quantity changes ($\mathrm{d}\ln \boldsymbol{Q}$) to recover the underlying bilateral cost shocks ($\mathrm{d}\ln \boldsymbol{Z}$), exploiting the invertibility of the linear sufficient statistics $\boldsymbol{G}$ in

[27] Kleinman et al. (2024) show that linearized counterfactuals in this class of trade models almost coincide with the nonlinear solution (e.g. see Dekle et al., 2008 and Caliendo et al., 2017) even for large shocks.

[28] While it is feasible to build upon Allen et al. (2020) to derive impacts on trade quantities, this specific derivation is not explicit in the existing literature. To clarify, the goal of our derivations is not to claim that Proposition 1 is groundbreaking, rather, it provides the specific result needed in our applied context to assess trade cost shocks and welfare impact based on changes in trade quantities, which is not directly available from prior studies.

Proposition 1, where we compute $\boldsymbol{G}$ using the trade elasticity θ and the observed expenditure share matrix $\boldsymbol{S}$ before the pandemic.

It is important to note that locking down one city can trigger bilateral shocks through heterogeneous responses to the lockdown across the other cities. While the reduced-form approach can only estimate the effects of city-level lockdown, our structural model is capable of recovering the full matrix of shocks to bilateral trade costs and productivities. Specifically, a lockdown in city i may affect the city's productivity (a_i), cost of exporting from city i (i.e., τ_{ni}), and the cost of importing by the city (i.e., τ_{in}). So, the structural approach provides a way to examine the validity of assuming lockdowns to be city-level shocks in the reduced-form approach. Regressing the full set of time-varying, bilateral composite shocks $\mathrm{d}\ln z_{ni}$ on exporter and importer-month fixed effects yields an R^2 of 0.85, suggesting that most variations of trade cost shocks are indeed at the city level.

We then linearly project the recovered composite cost shocks $\mathrm{d}\ln \boldsymbol{Z}$ onto city-level lockdown events to separately estimate the effect of partial and full-scale lockdowns on the within- and between-city trade costs. Specifically, we assume parametrized trade cost shocks as

$$\mathrm{d}\ln z_{ni,t} = \sum_{k\in\{h,l\}} \left(\beta^k \mathbf{1}(n \neq i) + \gamma^k \mathbf{1}(n = i)\right) D^k_{ni,t} + \varepsilon_{ni,t}, \tag{9}$$

where $\mathbf{1}(n \neq i)$ and $\mathbf{1}(n = i)$ are between- and within-city dummies that equal one if $n \neq i$ and $n = i$, respectively. The coefficient β^k captures the impact of lockdowns on between-city composite costs, while γ^k captures the impact on within-city composite costs. Like in our reduced-form approach (equation (3)), the term $F(s_{ni,t})$ can be added to control the severity of the pandemic in the city pair (n, i).

We estimate (β^k, γ^k) by minimizing the weighted sum of squared residuals between the observed and simulated trade flow quantity changes in the general equilibrium. Let $\Psi \equiv (\beta^h, \gamma^h, \beta^l, \gamma^l)$.

$$\hat{\Psi} = \arg\min_{\Psi} \sum_{ni,t} W_{ni} \left(\mathrm{d}\ln \hat{Q}_{ni,t}(\Psi) - \mathrm{d}\ln Q_{ni,t}\right)^2 \tag{10}$$

where $\mathrm{d}\ln Q_{ni,t}$ is the observed trade flow quantity change and $\mathrm{d}\ln \hat{Q}_{ni,t}(\Psi)$ is the simulated trade flow quantity change from our model given the value of Ψ and equation (9), W_{ni} is a city-pair weight. Different from equation (1), which examines the impact on bilateral trade flows between a city-pair when either the importer or the exporter along this trade route undergoes a lockdown, equation (10) exploits our theoretical result, Proposition 1, which inverts the entire matrix of bilateral trade cost shocks from the changes in the bilateral trade flows.

The first-order approach we adopt enables us to obtain a closed-form solution, where we obtain $\hat{\Psi}$ as coefficients of a weighted regression of changes in trade flow quantities (stacking

the matrix $\mathrm{d}\ln \boldsymbol{Q}$ as a vector) on a transformation of the $\boldsymbol{G}$ matrix in Proposition 1 adjusted for lockdown status.[29]

We provide details of the closed-form solution in the appendix.

In practice, we proxy $\mathrm{d}\ln Q_{ni,t}$, for $n \neq i$, by change in the truck flow from city i to n ($\mathrm{d}\ln q_{ni,t}$). Our assumption is that bilateral truck flows are proportional to bilateral trade quantities. Due to data constraints, we assume that truck loading factors remain unchanged in counterfactuals. The city-to-city truck flow data do not measure within-city trade. To proxy $\mathrm{d}\ln Q_{ii,t}$, we assume the within-city truck flow change to equal the average truck flow change on all routes connected to the city.

$$\mathrm{d}\ln Q_{ii,t} = \frac{\sum_{n\neq i} q_{ni,t}^{19}\, \mathrm{d}\ln q_{ni,t}}{\sum_{n\neq i} q_{ni,t}^{19}}. \tag{11}$$

where $q_{ni,t}^{19}$ denotes the truck flow between city i and city n in the same period t in 2019.[30] Last, we set W_{ni} equal to the weight ω_{ni} in the reduced-form approach.

Equipped with the estimates (β^k, γ^k) for $k \in \{l, h\}$, we can exploit the second part of Proposition 1. We will conduct both an accounting exercise, decomposing the local and spillover effects of lockdowns on the real income of any other city, and a counterfactual exercise, where we predict the real income effects of hypothetical lockdowns of varying stringency. We conduct these exercises in Section 6.

5.1 Results

We now turn to the structural approach. To obtain $\boldsymbol{G}$, we assume $\theta = 4$ and calibrate the expenditure shares to the official provincial input output table in 2012 (see Appendix A.7 for details).[31] Note that the structural approach distinguishes the direction of trade flow. The sample size, therefore, almost doubles that in the reduced-form approach.

The first column in Table 3 reports the structurally estimated β^k and γ^k by (10), assuming the cost specification (9). The between-city composite cost will increase by 0.24 log points if there is a full-scale lockdown in the city pair. The within-city trade flow change, $\mathrm{d}\ln Q_{ii,t}$, disciplines the effect of lockdown on the within-city composite cost. This allows the structural

[29] $\boldsymbol{G}$ is a sufficient statistic that maps trade cost shocks into changes in trade flow quantities and as defined in the appendix.

[30] The inferred changes are correlated with the changes in the number of visits to office buildings and shopping malls according to mobile phone location data in Chen et al. (2021a) (correlation 0.66 for 2020 Q1).

[31] The results under different values of θ and the expenditure shares implied by alternative IO tables imply similar real income effects. See Table A5 in the appendix. Note that in Proposition 1 welfare is independent of trade elasticity. However, trade elasticity influences our structural estimation of lockdown's impact on trade quantity and, consequently, the welfare results. This can be seen by our assumption on trade cost shocks in equation (9), where lockdown effects are parameterized by β^k and γ^k. Trade elasticity affects the structural estimates of β^k and γ^k, though the effects are small.

approach to identify γ^k. The estimates suggest a 0.39 log points increase in the within-city composite cost by a full-scale lockdown. In line with the results in Table 2, the effect of partial lockdown is much milder than full-scale lockdown. The increase in the between- and within composite cost is 0.04 and 0.08 log points, respectively.

Table 3: Effect of Lockdown on Composite Cost, Structural Estimates

	(1)	(2)	(3)	(4)	(5)
	D_{ni}^k			$\hat{D}_{ni}^k$	
Full-scale lockdown ($n \neq i$)	0.2415	0.2458	0.2179	0.5723	0.5238
	(0.0260)	(0.0261)	(0.0249)	(0.0298)	(0.0306)
Full-scale lockdown ($n = i$)	0.3913	0.3952	0.3643	0.9641	0.9061
	(0.0635)	(0.0636)	(0.0615)	(0.0675)	(0.0684)
Partial lockdown ($n \neq i$)	0.0449	0.0484	0.0273	0.1411	0.1028
	(0.0103)	(0.0103)	(0.0103)	(0.0231)	(0.0240)
Partial lockdown ($n = i$)	0.0809	0.0838	0.0593	0.2619	0.2125
	(0.0228)	(0.0227)	(0.0223)	(0.0541)	(0.0544)
COVID Dummy ($n \neq i$)		0.0090			
		(0.0021)			
COVID Dummy ($n = i$)		0.0116			
		(0.0042)			
$\ln(1 + \text{Case})$			0.0099		0.0086
			(0.0010)		(0.0009)
Time FE	YES	YES	YES	YES	YES
City pair FE	YES	YES	YES	YES	YES
City pair trend	YES	YES	YES	YES	YES
Observations	419533	419533	419533	419533	419533
R-squared	0.3628	0.3633	0.3654	0.3665	0.3684

Note: The first four rows report the effect of lockdown on the between- and within-city composite cost. $n \neq i$ and $n = i$ refer to between- and within-city. D_{ii}^k and $\hat{D}_{ii}^k$ are the city's lockdown measures. COVID Dummy equals one if the city pair $n \neq i$ ($n = i$) has new COVID cases and none of the cities have full-scale or partial lockdowns. The other specifications are the same as those for Table 2.

To make sense of the estimates, we derive a formula on the trade flow quantity changes in a partial equilibrium, where nominal wages are constant and lockdown in city n or i only

affects the goods price sold from i to n through the composite cost, but does not affect the other prices.

$$\mathrm{d}\ln Q^{p}_{ni,t} = -(\theta+1)\,\mathrm{d}\ln z_{ni,t} \tag{12}$$

where $\mathrm{d}\ln Q^{p}_{ni,t}$ denotes the trade flow quantity change in the partial equilibrium and $\mathrm{d}\ln z_{ni,t}$ is from equation (9). The estimated β^k and γ^k imply that a type-k lockdown will reduce the between- and within-city trade flows by $(\theta+1)\beta^k$ and $(\theta+1)\gamma^k$ percent, respectively, in the partial equilibrium. The effect of full-scale lockdown on the between-city trade flow implied by the estimated β^k in the partial equilibrium is substantially larger than that estimated by the reduced-form approach.[32] The effects of partial lockdown are more similar. Note that a lockdown will affect trade flows through two channels in the general equilibrium that are absent in the partial equilibrium. First, the lockdown will reduce nominal wage in the locked down city and amplify its effects on trade flows. Second, the lower nominal wage will reduce the goods price sold from the city and, therefore, dampen the effects on trade flows. Our results suggest that the second channel dominates the first in full-scale lockdown, implying that the general equilibrium effects moderate economic losses of full-scale lockdown.

As in the reduced-form approach, we add COVID dummy to control for community-level lockdown. The second column of Table 3 shows the results. Again, we find the effects of the community-level lockdown to be small and the estimates of β^k and γ^k are robust. We also add $F(s_{ni,t}) = b\ln(1+\mathrm{Case}_{ni,t})$ to the cost specification and structurally estimate b. The third column of Table 3 shows that the effects of full-scale lockdown become smaller after controlling for the number of COVID cases but remain large and significant. Adding the control has a larger effect on the estimates of partial lockdown, though. Both are consistent with the findings from the reduced-form approach.

As in the reduced-form approach, the estimated coefficients of $\hat{D}^k_{ni,t}$ are much larger (the last two columns of the table). In the next section, we will use the estimates to perform policy counterfactuals of one-month lockdowns.

6 The Economic Cost of Lockdown

In this section we quantify the economic implications of lockdown. We first derive a model-based accounting framework that isolates the effects of locking down a city on itself, any other city and the aggregate economy. The aggregate impacts will be further decomposed into local and spillover components. Finally, we will conduct several counterfactual exercises to illustrate the potential economic damage of a nationwide lockdown.[33]

[32] This result is robust to the choice of θ within reasonable range of 2 and 6.

[33] Our analysis is based on a static model and does not take intertemporal substitution into account. We do want to note that, anecdotally, because the lockdowns typically occurred suddenly without prior notice,

6.1 A Model-Based Accounting Framework

We apply Proposition 1, equation (9) and estimates in Column 5 of Table 3 to generate the city level real income changes caused by the lockdown of city i (assuming no lockdowns in other cities). Specifically,

$$\mathrm{d}\ln \boldsymbol{u}_n^{i,k} \equiv \frac{\partial \ln \boldsymbol{u}_n}{\partial \ln \boldsymbol{z}_{ii}}\gamma^k + \sum_{j\neq i}\left[\frac{\partial \ln \boldsymbol{u}_n}{\partial \ln \boldsymbol{z}_{ji}} + \frac{\partial \ln \boldsymbol{u}_n}{\partial \ln \boldsymbol{z}_{ij}}\right]\beta^k, \qquad \forall k = h, l, \tag{13}$$

where $\mathrm{d}\ln \boldsymbol{u}_n^{i,h}$ ($\mathrm{d}\ln \boldsymbol{u}_n^{i,l}$) measures the impact of type-k lockdown in city i on the real income of city n, taking into account the general equilibrium effects while shutting down the effects of lockdown elsewhere that apply to goods shipping from any cities besides i. The partial derivative $\partial \ln \boldsymbol{u}_n / \partial \ln z_{ji}$ captures the sensitivity of real income in city n to the composite cost for route (j, i). When $n = j$ ($n = i$), the partial derivative captures the importer's (exporter's) real income sensitivity to the route-specific composite cost shock; when $n \notin \{j, i\}$, the partial derivative captures the general equilibrium effect that propagate through the trade network across cities.[34] The lockdown of city i affects the composite cost of selling goods to itself, z_{ii}, and to the other cities, z_{ij} with $j \neq i$. So, the first term on the right-hand side of (13) is simply the effect of locking down city i on the city's real income, while the second term captures the general equilibrium effect of the lockdown through its effects on the real income of other cities.

The percentage change of the real national income caused by a type-k lockdown in city i can be expressed as a weighted average of the percentage change of local real income across cities:

$$\hat{\boldsymbol{u}}_{ag}^{i,k} \equiv \sum_{n=1}^{N} \mu_n \hat{\boldsymbol{u}}_n^{i,k}, \tag{14}$$

where $\hat{\boldsymbol{u}}_n^{i,k} = \exp(\mathrm{d}\ln \boldsymbol{u}_n^{i,k}) - 1$ and μ_n is city n's pre-shock real income share. Equation (14) can be further decomposed into two components: The effect on the real income of the city itself (local effect) and the effect on the real income of the other cities (spillover effect):

$$\hat{\boldsymbol{u}}_{ag}^{i,k} = \mu_i \hat{\boldsymbol{u}}_i^{i,k} + \hat{\boldsymbol{u}}_{so}^{i,k}. \tag{15}$$

where

$$\hat{\boldsymbol{u}}_{so}^{i,k} = \sum_{n\neq i} \mu_n \hat{\boldsymbol{u}}_n^{i,k}.$$

shortages of even basic consumption and necessity goods were widely reported in the news and social media throughout the lockdown periods, suggesting some limits to the scope of intertemporal substitution.

[34] Proposition 1 enables us to calculate the entire set of partial derivatives for any n, j, i as functions of the pre-shock bilateral trade flows.

6.2 Results

We use the full-scale lockdown of Shijiazhuang in January and February 2021 as an example. Figure 3 plots its effect on each city ($\hat{\boldsymbol{u}}_n^{i,h}$) in our model, assuming that no other cities are locked down at the same time. The real income of Shijiazhuang would decline by 60%. The real income losses for most of the other cities are negligible, though they can be larger than 0.2% for 20 cities. At the aggregate level, the lockdown reduces the real national income by 0.4%.

Figure 3: The Effects of Shijiazhuang Lockdown (%)

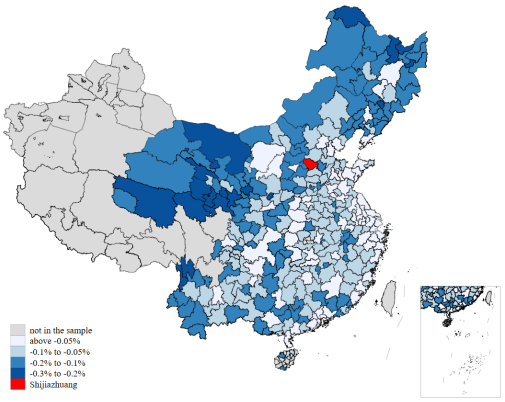

Note: The figure plots the effect of imposing full-scale lockdown on Shijiazhuang on each city's real come.

The left panel of Figure 4 plots the effect of imposing a full-scale one-month lockdown in a given city (with no lockdown in the other cities) on the real aggregate income ($\hat{\boldsymbol{u}}_{ag}^{i,h}, \forall i$). The largest three effects come from Shanghai, Beijing and Shenzhen, where full-scale lockdown will knock 2.7%, 2.5% and 1.9% off the real aggregate income, respectively. We decompose the effect of a full-scale lockdown on the real national income into local and spillover effects. The right panel of Figure 4 plots the contribution of spillover effects to the overall effects ($\hat{\boldsymbol{u}}_{so}^{i,h}/\hat{\boldsymbol{u}}_{ag}^{i,h}$, from equation (15)). The contribution of the spillover effects varies from 7 to 10 percent. If a one-month full-scale lockdown is imposed on the four largest cities in China (Beijing, Shanghai, Guangzhou, and Shenzhen), the four cities would lose their real income by 62% and the national real income would fall by 8.7%, of which 8.5% is contributed by the spillover effects. See Table A5 in the appendix for the result and its robustness.

The effect of locking down a city on the real national income is related to the city's economic size and its position in the network. To quantify the relative importance of the two factors, we regress $-\hat{\boldsymbol{u}}_{ag}^{i,h}$ on de-meaned city-level GDP and de-meaned eigenvector centrality derived from the city-to-city trade matrix excluding diagonal elements. Given the high correlation between

Figure 4: The Effect of Full-Scale Lockdown on the Real National Income

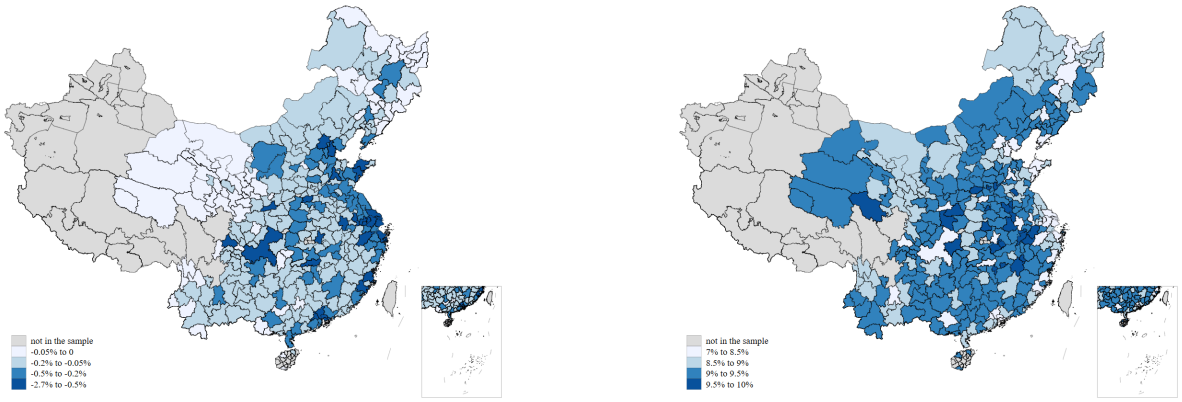

(a) Overall effect (b) Spillover effect

Note: The left panel plots the overall effect of imposing full-scale lockdown on each city on the real national income. The overall effect consists of local and spillover effects. The right panel plots the contribution of the spillover effect to the overall effect.

GDP and centrality measures, we employ Shapley Value regression. The results reveal that GDP and eigenvector centrality contribute almost equally to explaining variations in $-\hat{\boldsymbol{u}}_{ag}^{i,h}$, accounting for 51% and 49% respectively. Similar results hold for $-\hat{\boldsymbol{u}}_{so}^{i,h}$, where both GDP and eigenvector centrality explain half of the variations.

6.3 Economic Cost of Fighting Omicron

Lockdowns remained rare before the arrival of highly contagious Omicron variant. However, the rapid surge of Omicron infections in 2023 changed the landscape drastically. Many more cities were under lockdown for a much longer duration. Moreover, information about city-level lockdown became more scarce as public announcements of COVID policy were more specific to counties and districts. To estimate the scale of lockdowns during the Omicron surge, we apply the same approach to counties and districts with two modifications. We replace city with county/district and add "static management in all areas", a new euphemism for lockdown, to the keywords. We then manually select the official announcements about county/district-level lockdown from the scraped results. The left panel of Figure 5 shows the monthly population share of counties/districts under lockdown from January to June, 2022. In the first months of 2022, only 0.4% of China's population were under lockdown. The share increased sharply to 7.1% in March and further rose to the peak of 9.7% in May.

Using the effect of full-scale lockdown estimated from the pre-Omicron period, we can easily calculate aggregate welfare losses of the lockdowns in the Omicron surge implied by our model.

We assume the fraction of the locked down cities in our model, denoted by the set $\mathcal{A}_t$, to be the same as the share of the population under lockdown for each month t. The percentage change of the real national income caused by one-month full-scale lockdown in $\mathcal{A}_t$ follows

$$\widehat{\boldsymbol{U}}_t = \sum_{i \in \mathcal{A}_t} \mu_i \hat{\boldsymbol{u}}_{ag}^{i,h}, \tag{16}$$

where μ_i is city i's pre-shock real income share and $\hat{\boldsymbol{u}}_{ag}^{i,h}$ is the percentage change of the real national income caused by a full-scale lockdown in city i, which is defined in equation (14). The dotted line in the right panel of Figure 5 shows the results. Aggregate welfare drops by 10.4% and 10.6% in April and May, respectively.

Figure 5: Lockdown Share and Welfare Loss in 2022

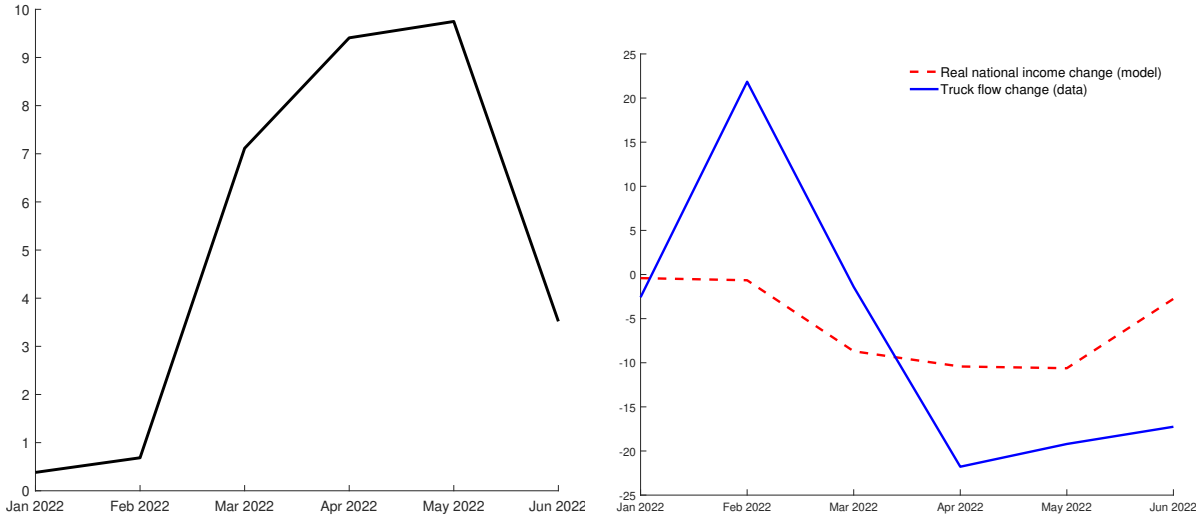

(a) Lockdown share (%) (b) Predicted and actual change (%)

Note: The left panel plots the population share of the counties and districts under lockdown. The dashed line in the right panel plots the change in aggregate welfare or, equivalently, total truck flows predicted by the model. The solid line plots the actual change in total truck flows in the data.

Interestingly, the actual declines in the truck flows (the solid line) in the two months are much larger than the prediction of the model. There are two possibilities. First, lockdowns in the Omicron surge were more strict than before and, therefore, inflicted larger economic costs. Second, we undercount the regions under lockdown. We cannot disentangle the two effects using the existing data and will have to leave it for future research.

7 Conclusion

This paper studies how China's lockdown policy that tries to "nip COVID-19 in the bud" causally affects city-to-city truck flows. Using a DiD design, we find that imposing full-scale lockdown on a city for a month halves the truck flows connected to the city in the month. While locking down one city has a small effect on the real national income in a large economy like China, implementing lockdown on a larger scale might cause significant economic losses. If a one-month full-scale lockdown is imposed on the four largest cities in China (Beijing, Shanghai, Guangzhou, and Shenzhen), the four cities would lose their real income by 62% and the real national income would fall by 8.7%, of which 8.5% is contributed by the spillover effects. The scenario was inconceivable before the emergence of Omicron in China. But in April and May of 2022, at least 9% of China's population (including Shanghai) were under lockdown, which translates into a 10% decline in the real national income in our model.

There are many reasons to believe that our estimates only capture the effects of lockdown in the short run. Its effects on expectations, saving and investment decisions in the longer term are all ignored in the current analysis. Moreover, our estimates alone do not provide evidence for or against immediate lockdowns in small COVID outbreaks, a central feature of China's zero-COVID policy. However, they may improve our understanding of the economic cost side of the policy and, therefore, help policymakers to balance the benefits and costs of lockdown.

References

Adams-Prassl, A., Boneva, T., Golin, M., Rauh, C., 2020. Inequality in the impact of the coronavirus shock: Evidence from real time surveys. Journal of Public Economics. 189, 104245.

Ahn, D., 2021. Lessons from non-pharmaceutical interventions on the first wave of COVID-19 in the asia pacific region. Journal of Global Health Science. 3 (1).

Ai, H., Zhong, T., Zhou, Z., 2022. The real economic costs of COVID-19: Insights from electricity consumption data in Hunan province, China. Energy Economics. 105, 105747.

Alder, S., Song, Z., Zhu, Z., 2023. On (un)congested roads: A quantitative analysis of infrastructure investment efficiency using truck gps data. Working Paper.

Alexander, D., Karger, E., 2023. Do stay-at-home orders cause people to stay at home? Effects of stay-at-home orders on consumer behavior. Review of Economics and Statistics. 105 (4), 1017–1027.

Allen, D. W., 2022. Covid-19 lockdown cost/benefits: A critical assessment of the literature. International Journal of the Economics of Business. 29 (1), 1–32.

Allen, T., Arkolakis, C., Takahashi, Y., 2020. Universal gravity. Journal of Political Economy. 128 (2), 393–433.

Altig, D., Baker, S., Barrero, J. M., Bloom, N., Bunn, P., Chen, S., Davis, S. J., Leather, J., Meyer, B., Mihaylov, E. et al., 2020. Economic uncertainty before and during the COVID-19 pandemic. Journal of Public Economics. 191, 104274.

Alvarez, F. E., Argente, D., Lippi, F., 2020. A simple planning problem for COVID-19 lockdown. NBER Working Paper No. 26981.

Andersen, A. L., Hansen, E. T., Johannesen, N., Sheridan, A., 2020. Pandemic, shutdown and consumer spending: Lessons from scandinavian policy responses to covid-19. Working paper arXiv:2005.04630.

Arkolakis, C., Costinot, A., Rodríguez-Clare, A., 2012. New trade models, same old gains? American Economic Review. 102 (1), 94–130.

Armington, P. S., 1969. A theory of demand for products distinguished by place of production. IMF Staff Papers. 16 (1), 159–178.

Atkeson, A., 2020. What will be the economic impact of COVID-19 in the US? Rough estimates of disease scenarios. NBER Working Paper No. 26867.

Atkeson, A., Kopecky, K., Zha, T., 2020. Four stylized facts about COVID-19. NBER Working Paper No. 27719.

Aum, S., Lee, S. Y. T., Shin, Y., 2021. Inequality of fear and self-quarantine: Is there a trade-off between GDP and public health? Journal of Public Economics. 194, 104354.

Auray, S., Eyquem, A., 2020. The macroeconomic effects of lockdown policies. Journal of Public Economics. 190, 104260.

Baker, A. C., Larcker, D. F., Wang, C. C., 2022. How much should we trust staggered difference-in-differences estimates? Journal of Financial Economics. 144 (2), 370–395.

Baqaee, D., Farhi, E., 2020. Supply and demand in disaggregated keynesian economies with an application to the COVID-19 crisis. NBER Working Paper No. 27152.

Barrero, J. M., Bloom, N., Davis, S. J., 2021. Why working from home will stick. NBER Working Paper No. 28731.

Bartik, A. W., Bertrand, M., Cullen, Z. B., Glaeser, E. L., Luca, M., Stanton, C. T., 2020. How are small businesses adjusting to COVID-19? Early evidence from a survey. NBER Working Paper No. 26989.

Bendavid, E., Oh, C., Bhattacharya, J., Ioannidis, J. P. A., 2021. Assessing mandatory stay-at-home and business closure effects on the spread of COVID-19. European Journal of Clinical Investigation. 51 (4), e13484.

Berry, C. R., Fowler, A., Glazer, T., Handel-Meyer, S., MacMillen, A., 2021. Evaluating the effects of shelter-in-place policies during the COVID-19 pandemic. Proceedings of the National Academy of Sciences. 118 (15), e2019706118.

Birinci, S., Karahan, F., Mercan, Y., See, K., 2021. Labor market policies during an epidemic. Journal of Public Economics. 194, 104348.

Bonadio, B., Huo, Z., Levchenko, A. A., Pandalai-Nayar, N., 2020. Global supply chains in the pandemic. NBER Working Paper No. 27224.

Brodeur, A., Clark, A. E., Fleche, S., Powdthavee, N., 2021. COVID-19, lockdowns and well-being: Evidence from google trends. Journal of Public Economics. 193, 104346.

Buechler, E., Powell, S., Sun, T., Astier, N., Zanocco, C., Bolorinos, J., Flora, J., Boudet, H., Rajagopal, R., 2022. Global changes in electricity consumption during COVID-19. iScience. 25 (1), 103568.

Buera, F. J., Oberfield, E., 2020. The global diffusion of ideas. Econometrica. 88 (1), 83–114.

Caliendo, L., Parro, F., Tsyvinski, A., 2017. Distortions and the structure of the world economy. NBER Working Paper No. 23332.

Cameron, A. C., Gelbach, J. B., Miller, D. L., 2011. Robust inference with multiway clustering. Journal of Business & Economic Statistics. 29 (2), 238–249.

Carrère, C., Mrázová, M., Neary, J. P., 2020. Gravity without apology: The science of elasticities, distance and trade. Economic Journal. 130 (628), 880–910.

de Chaisemartin, C., D'Haultfœuille, X., 2020. Two-way fixed effects estimators with heterogeneous treatment effects. American Economic Review. 110 (9), 2964–96.

Chen, H., Qian, W., Wen, Q., 2021. The impact of the COVID-19 pandemic on consumption: Learning from high-frequency transaction data. AEA Papers and Proceedings. 111, 307–11.

Chen, Q., He, Z., Hsieh, C., Song, Z., 2021a. Economic effects of lockdown in China. In: Impact of COVID-19 on Asian Economies and Policy Responses. 3–10, World Scientific.

Chen, Q., Rodewald, L., Lai, S., Gao, G. F., 2021b. Rapid and sustained containment of COVID-19 is achievable and worthwhile: Implications for pandemic response. BMJ. 375.

Chetty, R., Friedman, J. N., Hendren, N., Stepner, M., 2020. How did COVID-19 and stabilization policies affect spending and employment? A new real-time economic tracker based on private sector data. NBER Working Paper No. 27431.

CICC, 2020. Production activity index. China International Capital Corporation.

Coibion, O., Gorodnichenko, Y., Weber, M., 2020. The cost of the COVID-19 crisis: Lockdowns, macroeconomic expectations, and consumer spending. NBER Working Paper No. 27141.

Dekle, R., Eaton, J., Kortum, S., 2008. Global rebalancing with gravity: Measuring the burden of adjustment. IMF Staff Papers. 55 (3), 511–540.

Diewert, W. E., Fox, K. J., 2020. Measuring real consumption and CPI bias under lockdown conditions. NBER Working Paper No. 27144.

Dingel, J. I., Neiman, B., 2020. How many jobs can be done at home? Journal of Public Economics. 189, 104235.

Eaton, J., Kortum, S., 2002. Technology, geography, and trade. Econometrica. 70 (5), 1741–1779.

Eaton, J., Kortum, S., Neiman, B., Romalis, J., 2016. Trade and the global recession. American Economic Review. 106 (11), 3401–3438.

Eichenbaum, M. S., Rebelo, S., Trabandt, M., 2021. The macroeconomics of epidemics. Review of Financial Studies. 34 (11), 5149–5187.

Eppinger, B., Zigan, L., Karl, J., Will, S., 2020. Pumped thermal energy storage with heat pump-orc-systems: Comparison of latent and sensible thermal storages for various fluids. Applied Energy. 280, 115940.

Fang, H., Wang, L., Yang, Y., 2020. Human mobility restrictions and the spread of the novel coronavirus (2019-ncov) in China. Journal of Public Economics. 191, 104272.

Forsythe, E., Kahn, L. B., Lange, F., Wiczer, D., 2020. Labor demand in the time of COVID-19: Evidence from vacancy postings and UI claims. Journal of Public Economics. 189, 104238.

Gao, Y., Li, M., Lu, Y., 2020. What can be learned from billions of invoices? The construction and application of China's multiregional input-output table based on big data from the value-added tax. Emerging Markets Finance and Trade. 56 (9), 1925–1941.

Goodman-Bacon, A., 2021. Difference-in-differences with variation in treatment timing. Journal of Econometrics. 225 (2), 254–277.

Goolsbee, A., Syverson, C., 2021. Fear, lockdown, and diversion: Comparing drivers of pandemic economic decline 2020. Journal of Public Economics. 193, 104311.

Gottlieb, C., Grobovšek, J., Poschke, M., Saltiel, F., 2022. Lockdown accounting. The B.E. Journal of Macroeconomics. 22 (1), 197–210.

Guerrieri, V., Lorenzoni, G., Straub, L., Werning, I., 2020. Macroeconomic implications of COVID-19: Can negative supply shocks cause demand shortages? NBER Working Paper No. 26918.

Hale, T., Cameron-Blake, E., Folco, M. D., Furst, R., Green, K., Phillips, T., Sudarmawan, A., Tatlow, H., Zha, H., 2022a. What have we learned from tracking every government policy on COVID-19 for the past two years? BSG Working Paper.

Hale, T., Petherick, A., Phillips, T., Webster, S., 2020. Variation in government responses to COVID-19. BSG Working Paper.

Hale, T., Zhang, Y., Zha, H., Zhou, H., Wang, L., Zhang, Z., Tan, Z., Deng, L., 2022b. Chinese provincial government responses to COVID-19. BSG Working Paper.

Hanna, R., Kreindler, G., Olken, B. A., 2017. Citywide effects of high-occupancy vehicle restrictions: Evidence from "three-in-one" in Jakarta. Science. 357 (6346), 89–93.

He, G., Pan, Y., Tanaka, T., 2020. The short-term impacts of COVID-19 lockdown on urban air pollution in China. Nature Sustainability. 3 (12), 1005–1011.

Head, K., Ries, J., 2001. Increasing returns versus national product differentiation as an explanation for the pattern of U.S.-Canada trade. American Economic Review. 91 (4), 858–876.

Hensvik, L., Le Barbanchon, T., Rathelot, R., 2021. Job search during the COVID-19 crisis. Journal of Public Economics. 194, 104349.

Hsu, W., Lin, H., Yang, H., 2020. Between lives and economy: Optimal COVID-19 containment policy in open economies. SMU Economics and Statistics Working Paper No. 10-2020.

Kleinman, B., Liu, E., Redding, S. J., 2024. International friends and enemies. American Economic Journal: Macroeconomics. 16 (4), 350–385.

Krueger, D., Uhlig, H., Xie, T., 2020. Macroeconomic dynamics and reallocation in an epidemic: Evaluating the "Swedish solution". NBER Working Paper No. 27047.

Lazarus, J. V., Ratzan, S., Palayew, A., Billari, F. C., Binagwaho, A., Kimball, S., Larson, H. J., Melegaro, A., Rabin, K., White, T. M. et al., 2020. COVID-score: A global survey to assess public perceptions of government responses to COVID-19 (COVID-SCORE-10). PloS one. 15, e0240011.

Liu, W., Tang, Z., Han, M. et al., 2018. The 2012 China multi-regional input–output table of 31 provincial units. Beijing: China Statistics Press.

Luo, J., 2020. Input-output analysis and application based on VAT invoice data. Manucript.

Maliszewska, M., Mattoo, A., Van Der Mensbrugghe, D., 2020. The potential impact of COVID-19 on GDP and trade: A preliminary assessment. World Bank Policy Research Working Paper No. 9211.

Montenovo, L., Jiang, X., Rojas, F. L., Schmutte, I. M., Simon, K. I., Weinberg, B. A., Wing, C., 2020. Determinants of disparities in COVID-19 job losses. NBER Working Paper No. 27132.

Ou, J., Meng, J., Zheng, H., Mi, Z., Shan, Y., Guan, D., 2019. Frequent interactions of Tibet's CO2 emissions with those of other regions in China. Earth's Future. 7 (4), 491–502.

Palomino, J. C., Rodríguez, J. G., Sebastian, R., 2020. Wage inequality and poverty effects of lockdown and social distancing in Europe. European Economic Review. 129, 103564.

Pei, J., de Vries, G., Zhang, M., 2022. International trade and COVID-19: City-level evidence from China's lockdown policy. Journal of Regional Science. 62 (3), 670–695.

Tang, J., Li, L., 2021. Importance of public health tools in emerging infectious diseases. BMJ. 375.

Zheng, H., Zhang, Z., Wei, W., Song, M., Dietzenbacher, E., Wang, X., Meng, J., Shan, Y., Ou, J., Guan, D., 2020. Regional determinants of China's consumption-based emissions in the economic transition. Environmental Research Letters. 15 (074001).

A Appendix

A.1 Lockdown Events

Table A1 and Table A2 below list all identified full-scale lockdowns and partial lockdowns, respectively.

Table A1: Full-Scale Lockdowns

City	Starting date	Ending date	Lockdown days	COVID Cases	Δ Truck Flow
Jilin	2020/5/13	2020/6/7	26	44 (12.1)	-0.38
Shijiangzhuang	2021/1/7	2021/1/29	23	865 (77)	-0.73
Langfang	2021/1/12	2021/1/16	5	1 (0.2)	-0.29
Suihua	2021/1/12	2021/2/6	26	489 (130.2)	-0.59
Xingtai	2021/1/12	2021/1/16	5	71 (10)	-0.74
Tonghua	2021/1/15	2021/2/21	38	307 (235.6)	-0.25
Songyuan	2021/1/20	2021/2/3*	15	4 (1.8)	-0.23
Lu'an	2021/5/18	2021/6/8	22	8 (1.8)	-0.001
Yangzhou	2021/7/31	2021/9/3	35	570 (125)	-0.51
Zhangjiajie	2021/8/1	2021/8/25	25	67 (44.2)	-1.24
Zhuzhou	2021/8/1	2021/8/20	20	29 (7.4)	-0.20
Jiayuguan	2021/10/23	2021/11/4*	13	5 (15.9)	-0.12
Zhangye	2021/10/23	2021/11/19	28	15 (13.3)	-0.06
Heihe	2021/10/28	2021/12/22	56	271 (210.7)	-0.16
Xi'an	2021/12/23	2022/1/15	24	2052 (158.3)	-0.75
Anyang	2022/1/10	2022/1/31*	22	465 (84.9)	-0.62

Note: The definitions are the same as Table 1. The ending date with * is inferred from lockdown ended 7 days prior to the "clearance" day or the end of our sample period (2022/1/31).

Table A2: Partial Lockdowns

City	Starting date	Ending date	Lockdown days	COVID Cases	Δ Truck Flow
Baoding	2020/6/18	2020/7/2*	15	16 (1.4)	-0.09
Dehong	2020/9/14	2020/9/21	8	0 (0)	0.06
Dehong	2021/7/7	2021/7/25	19	88 (66.9)	-0.17
Dehong	2021/3/30	2021/4/26	28	93 (70.7)	0.06
Qiqihaer	2021/1/12	2021/2/7	27	1 (0.2)	-0.05
Haerbin	2021/9/24	2021/10/13*	20	89 (8.9)	-0.03
Haerbin	2021/12/8	2021/12/17	10	42 (4.2)	-0.18
Haerbin	2021/1/18	2021/2/12*	26	146 (14.6)	-0.13
Huaian	2021/7/29	2021/8/16	19	12 (2.6)	-0.12
Xiangxi	2021/8/1	2021/8/7*	7	0 (0)	-0.60
Jingmen	2021/8/7	2021/8/23	17	43 (16.6)	-0.48
Tianshui	2021/10/27	2021/11/25	30	39 (13.1)	-0.61
Zhoukou	2021/11/4	2021/11/25	22	18 (2)	-0.10
Hulunbeier	2021/11/27	2021/12/25	29	558 (249.5)	-0.33
Shaoxing	2021/12/11	2021/12/31	21	387 (73.1)	-0.31
Fangchenggang	2021/12/22	2022/1/8	18	20 (19.1)	-0.21
Xianyang	2021/12/23	2022/1/20	29	15 (3.8)	-0.58
Weinan	2021/12/26	2022/1/9	15	1 (0.2)	-0.61
Xuchang	2022/1/2	2022/1/31*	30	365 (83.3)	-0.11
Yan'an	2022/1/3	2022/1/13	11	2 (0.9)	-0.58
Xinyang	2022/1/12	2022/1/16	5	3 (0.5)	-0.32
Mudanjiang	2022/1/26	2022/1/31*	6	4 (1.7)	-0.16

Note: The definitions are the same as Table 1. The ending date with * is inferred from lockdown ended 7 days prior to the "clearance" day or the end of our sample period (2022/1/31).

A.2 Robustness Check of DiD results

The recent literature shows that the two-way fixed effects (TWFE) estimator is equal to a weighted sum of the treatment effect in each treated cell, where some weights may be negative. The negative weights are an issue when the treatment effects are heterogeneous across groups or periods. de Chaisemartin and D'Haultfœuille (2020) suggest a diagnosis by checking the weights attached to the TWFE regressions and the absolute value of the coefficient relative to the standard deviation of the weights. If many weights are negative and the ratio is not very large, the TWFE estimator is likely biased. They also propose a new estimator, "DID_{M}", which is valid even with treatment effect heterogeneity. It estimates the average treatment effect across all the cells whose treatment changes from $t-1$ to t. A test for pretrends is provided.[35]

[35] Goodman-Bacon (2021) and Baker et al. (2022) also propose similar estimators to correct the potential bias of the TWFE regressions.

Table A3: Robustness Check of the Lockdown Effects

	Two-way fixed effects		Joiners' effect in "DID_M"	
	(1)	(2)	(3)	(4)
2 periods before full-scale lockdown	-0.0019		-0.0319	
	(0.0164)		(0.0195)	
1 period before full-scale lockdown	0.0300		0.0351	
	(0.0182)		(0.0180)	
Full-scale lockdown	-0.4028		-0.4422	
	(0.0458)		(0.0512)	
2 periods before partial lockdown		0.0314		-0.0103
		(0.0356)		(0.0247)
1 period before partial lockdown		-0.0078		-0.0442
		(0.0264)		(0.0296)
Partial lockdown		-0.0931		-0.0901
		(0.0293)		(0.0193)
Time FE	YES	YES	YES	YES
City pair FE	YES	YES	YES	YES
City pair trend	YES	YES	YES	YES
Observations	204939	204910	204939	204910

Note: The first two columns report the TWFE estimators. The last two columns report the estimated joiners' effects using de Chaisemartin and D'Haultfœuille (2020).

Note that "DID_M" estimates both the joiners' and leavers' treatment effects. The joiners' treatment effect compares the evolution of the mean outcome between $t-1$ and t in two sets of groups: the joiners (a group from untreated to treated) and those remaining untreated. The leavers' treatment effect compares the evolution of the mean outcome between $t-1$ and t between the leavers (a group from treated to untreated) and those remaining treated. Since we have few observations that have been treated in two consecutive periods, the control group for leavers, we choose to estimate the joiners' effect only.

To make the TWFE estimator be entirely comparable to that for the joiners' effect in "DID_M", we only keep the observations at T_0 for each lockdown period $[T_0, T_1]$. This drops 721 observations with lockdown in total.[36] Reassuringly, we find no negative weights in our TWFE regressions. Table A3 compares the TWFE estimators (column 1 and 2, which are very close

[36]Keeping the observations in the sample would lead to essentially the same results.

to those in the text) and those by "DID_M" (column 3 and 4). Both methods show no evidence for pretrends. The point estimates are also very similar.

A.3 Robustness Check of City-Specific Time-Varying Shocks

In the first robustness check, we estimate exporter- and importer-time fixed effects from

$$\mathrm{d}\ln q_{ni,t} = \gamma_{i,t} + \pi_{n,t} + \delta_{ni} + \epsilon_{ni,t}, \tag{17}$$

where $\gamma_{i,t}$ and $\pi_{n,t}$ are the exporter- and importer-time fixed effects. We then estimate the effect of lockdown on the fixed effects. In the event study, we replace $\mathrm{d}\ln q_{ni,t}$ with $\hat{\gamma}_{i,t} + \hat{\pi}_{n,t}$ as the dependent variable.

$$\hat{\gamma}_{i,t} + \hat{\pi}_{n,t} = \sum_{k\in\{h,l\}} \left(\sum_{j=1}^{\bar{J}} \alpha^k_{-j} PRE^{k,j}_{ni,t} + \alpha^k_0 D^k_{ni,t} + \sum_{j=1}^{\bar{J}} \alpha^k_j POST^{k,j}_{ni,t} \right) + \delta_{ni} + \nu_t + \eta_{ni} t + \epsilon_{ni,t}. \tag{18}$$

The results are plotted in Figure A1. The estimated effect of full-scale and partial lockdown is -0.37 and -0.10 log points, close to the estimates of -0.41 and -0.10 log points in the benchmark case.

Figure A1: Event Study: Importer- and Exporter-Time Fixed Effects

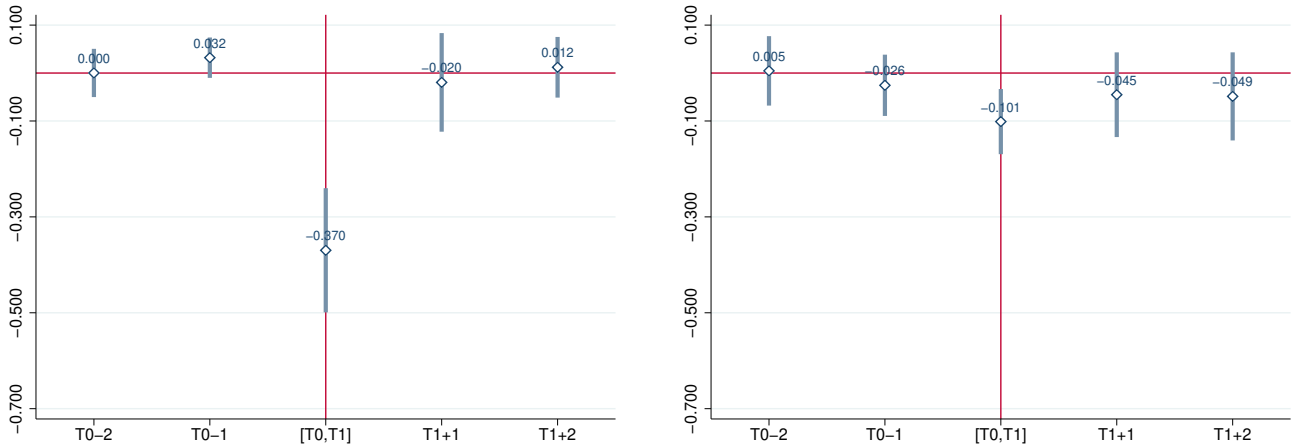

(a) Full-scale lockdown

(b) Partial lockdown

Note: The figure plots the estimated α^h_j (left panel) and α^l_j (right panel) in equation (18), together with their 95% confidence intervals.

In the second robustness check, we interact exporter and importer dummies with year or semi-year dummies to control for the city-specific characteristics that vary at lower frequency

as in (19). The dummies are added to the event study. Our results are robust.

$$\begin{aligned} \mathrm{d}\ln q^{s}_{ni,t} \quad = \quad & \sum_{k\in\{h,l\}} \left(\sum_{j=1}^{\bar{J}} \alpha^{k}_{-j} PRE^{k,j}_{ni,t} + \alpha^{k}_{0} D^{k}_{ni,t} + \sum_{j=1}^{\bar{J}} \alpha^{k}_{j} POST^{k,j}_{ni,t} \right) \\ & + \delta_{ni} + \nu_{t} + \eta_{ni} t + \gamma_{i,s} + \pi_{n,s} + \epsilon_{ni,t}, \end{aligned} \tag{19}$$

where s denotes the year or semi-year; $\gamma_{i,s}$ and $\pi_{n,s}$ are the exporter and importer dummies interacted with year or semi-year dummies, respectively.

Figure A2: Event Study Controlling for Exporter- and Importer Fixed Effects Interacted with Semi-Year or Year Dummies

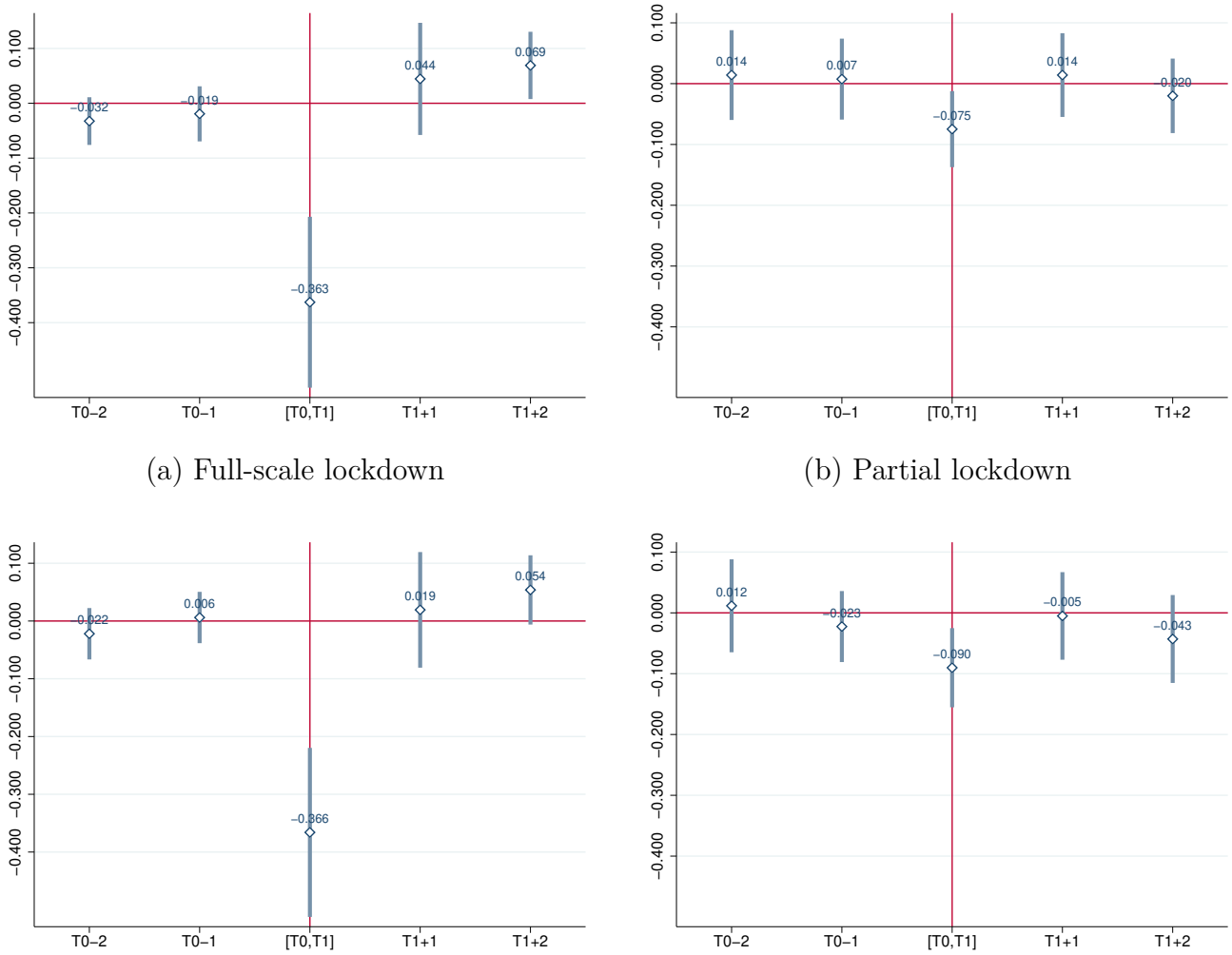

(a) Full-scale lockdown

(b) Partial lockdown

(c) Full-scale lockdown

(d) Partial lockdown

Note: The figure plots the estimated α^{h}_{j} (left panels) and α^{l}_{j} (right panels) in equation (19). The top (bottom) panels control for the exporter- and importer fixed effects interacted with semi-year (year) dummies.

A.4 Robustness Check of City-Level Regression

We run the following city-month-level regression.

$$\mathrm{d}\ln q_{i,t} = \sum_{k\in\{h,l\}} \beta^k C^k_{i,t} + \delta_i + \nu_t + \eta_i t + \epsilon_{i,t}, \tag{20}$$

where $C^k_{i,t}$ is a city-specific lockdown dummy.

$$C^k_{i,t} = \begin{cases} 1 & \text{if type-}k\text{ lockdown in city } i \text{ at } t \\ 0 & \text{otherwise} \end{cases} \tag{21}$$

For illustrative purpose, We write our lockdown dummy $D^k_{ni,t}$ as a function of $C^k_{i,t}$:

$$D^k_{ni,t} = C^k_{i,t} + C^k_{n,t}. \tag{22}$$

Since double lockdowns (i.e., both city i and n are under lockdown) are rare, we ignore $C^k_{i,t} \times C^{k'}_{n,t}$ for simplicity.

We next use the main specification (1) to aggregate the change in bilateral truck flows to the city level.

$$\begin{aligned} \mathrm{d}\ln q_{i,t} &\equiv \sum_{n\neq i} w_{ni}\, \mathrm{d}\ln q_{ni,t} \\ &= \sum_{n\neq i} w_{ni} \left(\alpha^k \sum_{k\in\{h,l\}} D^k_{ni,t} + \delta_{ni} + \nu_t + \eta_{ni} t + \epsilon_{ni,t} \right) \\ &= \sum_{k\in\{h,l\}} \alpha^k C^k_{i,t} + \underbrace{\sum_{k\in\{h,l\}} \alpha^k \sum_{n\neq i} w_{ni} C^k_{n,t}}_{\text{the term missing in (20)}} + \delta_i + \nu_t + \eta_i t + \sum_{n\neq i} w_{ni}\epsilon_{ni,t}, \end{aligned} \tag{23}$$

where w_{ni} is the share of exports from i to n in total exports of i in 2019. Compared with equation (23) aggregated from the route-level regression, the city-level regression (20) omits $\sum_{n\neq i} \alpha^k w_{ni} C^k_{n,t}$ – i.e., the effects of locking down city i's importers on its exports. The omitted terms do not affect the treatment group ($C^k_{i,t} = 1$ and $C^k_{n,t} = 1$ for $n \neq i$ are mutually exclusive without double lockdown). However, the control group is affected. Locking down city i will affect the cities in the control group that export to city i.

We then generalize (20) to the event-study approach.

$$\mathrm{d}\ln q_{i,t} = \sum_{k\in\{h,l\}} \left(\sum_{j=1}^{\bar{J}} \beta^k_{-j} PRE^{k,j}_{i,t} + \beta^k_0 C^k_{i,t} + \sum_{j=1}^{\bar{J}} \beta^k_j POST^{k,j}_{i,t} \right) + \delta_i + \nu_t + \eta_i t + \epsilon_{i,t}. \tag{24}$$

To be consistent with our specification, we use the sample without double lockdowns.[37] Figure A3 shows the results. We also apply route-level regression to the same sample. As expected, the estimated effect of major lockdown reduces from 0.387 using route-level regression to 0.373 using city-level regression. The effect of minor lockdown is essentially the same. The simpler city-level regression gives quantitatively similar estimates.

Figure A3: Event Study at City Level

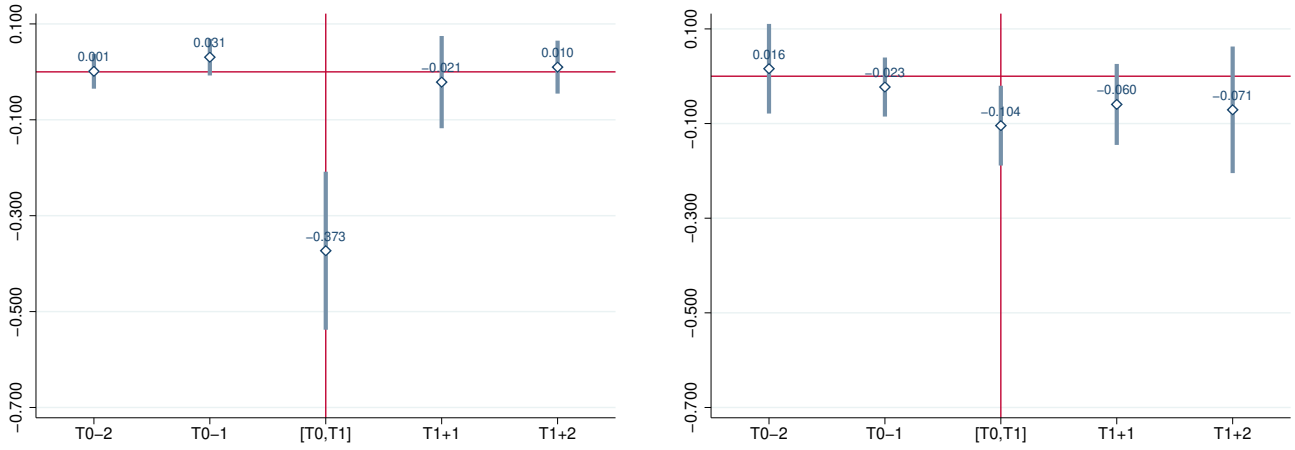

(a) Full-scale lockdown

(b) Partial lockdown

Note: The figure plots the estimated β_j^h (left panel) and β_j^l (right panel) in equation (24), together with their 95% confidence intervals.

A.5 Violation of SUTVA

Figure A4 plots the results for different control groups. The top and middle panels show that the effects of full-scale and partial lockdown are only slightly affected by more restrictive control groups. The bottom panels show our results are also robust to controls of lockdowns along the routes.

[37] Note that there are only 8 observations of double full-scale lockdown, compared with 1,017 observations of single full-scale lockdown.

Figure A4: Event Study: Robustness Checks

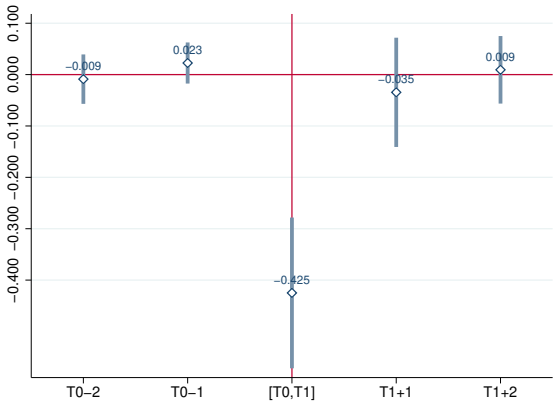

(a) Full-scale lockdown (w/o neighbors)

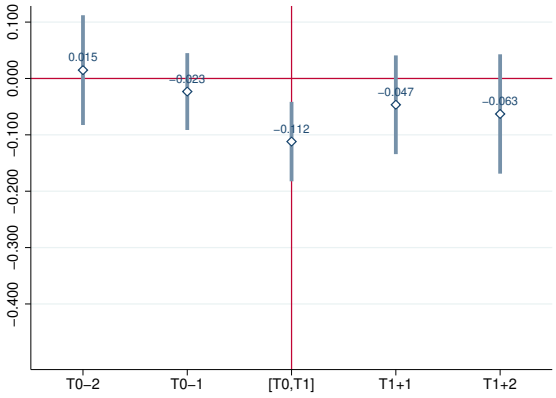

(b) Partial lockdown (w/o neighbors)

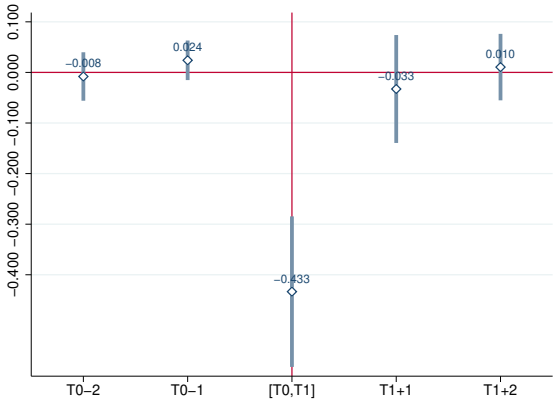

(c) Full-scale lockdown (w/o important trading partners)

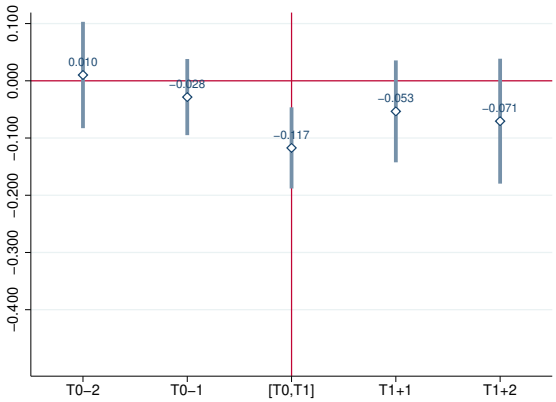

(d) Partial lockdown (w/o important trading partners)

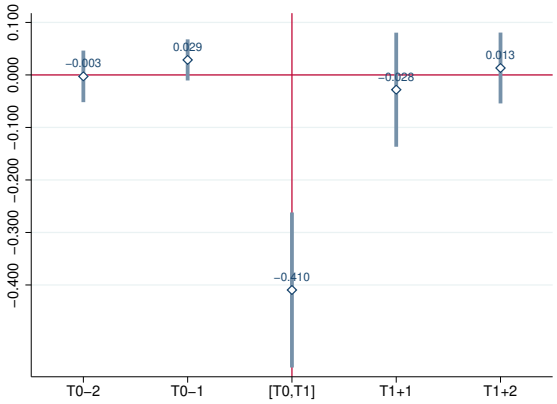

(e) Full-scale lockdown (w/o lockdown along the route)

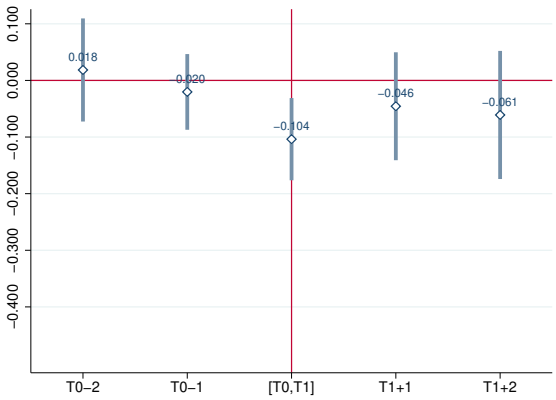

(f) Partial lockdown (w/o city pairs with lockdown along the route)

Note: The figure plots the estimated α_j^h (left panel) and α_j^l (right panel) in (1) of the paper with a "cleaner" control group, together with their 95% confidence intervals. The top, middle, and bottom panels exclude neighbors, important trading partners, and city pairs with lockdown along the route, respectively.

The specification for route-specific regression is

$$\mathrm{d}\ln q_{ni,t} = \sum_{k\in\{h,l\}} \alpha^k D^k_{ni,t} + \delta_{ni} + \eta_{ni} t + \epsilon_{ni,t}. \tag{25}$$

The distribution of the estimated values of α^k across city pairs are shown in Figure A5. The average, weighted by the corresponding route's total truck flows in 2019, is -0.38 and -0.15 for full-scale and partial lockdown, respectively.[38]

Figure A5: Distribution of the Estimated Values of α^k

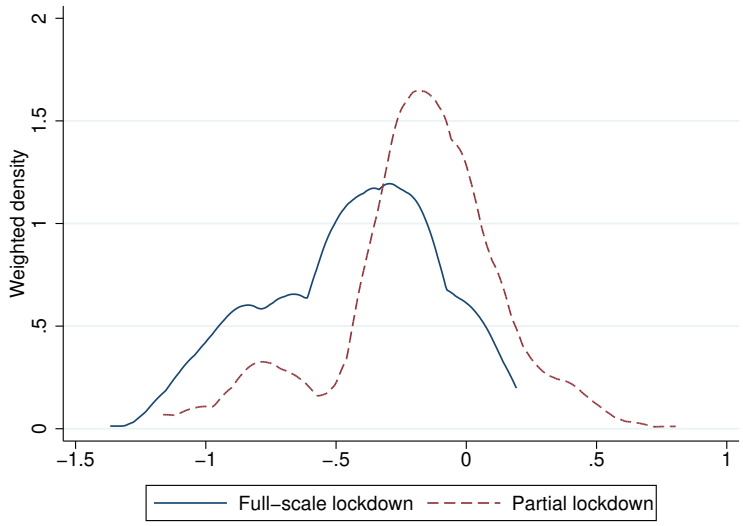

Note: The figure plots the distribution of the estimated α^h_j (solid line) and α^l_j (dashed line) in equation (25). Each observation's density is weighted by the corresponding route's total truck flows in 2019.

To test the substitutability of truck flows between the city that is under lockdown and the other cities that are not, we construct a variable for city i that measures the change in total truck flows to its neighboring cities but excludes the change in truck flows from city i.

$$\mathrm{d}\ln q^{neighbor}_{i,t} \equiv \sum_{j\in\mathcal{N}_i \;\&\; C^k_{j,t}=0} W^i_{j,t} \sum_{n\neq i \;\&\; C^k_{n,t}=0} w^i_{jn,t}\, \mathrm{d}\ln q_{jn,t}, \tag{26}$$

where $\mathcal{N}_i$ is the set of city i's neighboring cities, $W^i_{j,t}$ is city j's truck flow share in city i's neighboring and non-locked down cities, $w^i_{jn,t}$ is route jn's truck flow share in all non-locked down routes connected to city j (also excluding the route ji), $C^k_{n,t}$ and $C^k_{j,t}$ are lockdown dummy variables as defined in equation (21).

[38]The weighted standard deviation is 0.17 and 0.25 for full-scale and partial lockdown, respectively.

If city i's trading partners can easily switch to another city, locking down city i should lead to an increase in truck flows to its neighbors from cities other than i. We test the hypothesis in the following event study.

$$\mathrm{d}\ln q_{i,t}^{neighbor} = \sum_{k\in\{h,l\}} \left(\sum_{j=1}^{\bar{J}} \beta_{-j}^{k} PRE_{i,t}^{k,j} + \beta_{0}^{k} C_{i,t}^{k} + \sum_{j=1}^{\bar{J}} \beta_{j}^{k} POST_{i,t}^{k,j} \right) + \delta_i + \nu_t + \eta_i t + \epsilon_{i,t}, \quad (27)$$

Figure A6 plots the estimation results. The effects on $\mathrm{d}\ln q_{i,t}^{neighbor}$ are small and insignificant.

Figure A6: Effects of Lockdown on Neighboring Cities

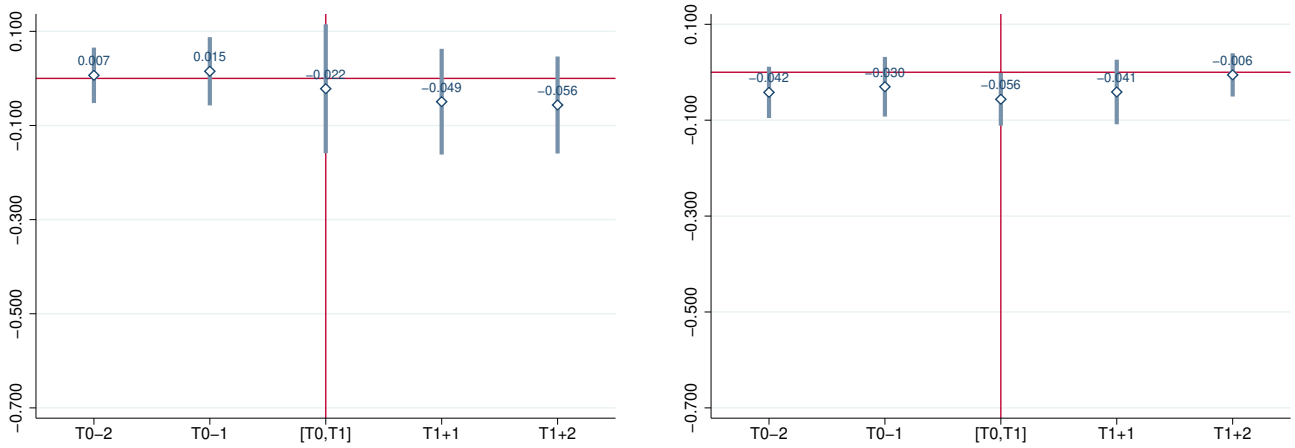

(a) Full-scale lockdown

(b) Partial lockdown

Note: The figure plots the estimated β_j^h (left panel) and β_j^l (right panel) in equation (27), together with their 95% confidence intervals.

A.6 City-to-City Population Flows

Following Fang et al. (2020), we use two population flow indicators from Baidu Migration Index (BMI, `https://qianxi.baidu.com`): city-level daily in- and out-migration index, denoted by $IM_{i,t}$ and $OM_{i,t}$, respectively. According to Baidu's definition, these two indices are comparable across cities and over time. The data covers 364 Chinese cities in the Chinese new year period (i.e., 24 days before and 36 days after the Chinese new year by the lunar calendar) in 2019 and 2020, and the periods of April-June and September-December in 2020, and the whole period after January 19, 2021.

BMI also provides the share of inflows, denoted by $IMS_{ni,t}$, from the top 100 origination cities (i) to each of the 364 cities (n) and the share of outflows, denoted by $OMS_{ni,t}$, to the top 100 destination cities (n) from each of the 364 cities (i). Two remarks are in order. First, the population inflows from and outflows to the top 100 origination and destination cities account

for 97% of the total population flows in BMI. Second, Both $IM_{n,t} \times IMS_{ni,t}$ and $OM_{i,t} \times OMS_{ni,t}$ measure the population flow from city i to city n and, therefore, should be identical. Yet, we find small differences between the two measures in 2019.[39] So we take average to get $Flow_{ni,t}$, the index for population flow from i to n:

$$Flow_{ni,t} = \frac{1}{2}(IM_{n,t} \times IMS_{ni,t} + OM_{i,t} \times OMS_{ni,t}). \tag{28}$$

We benchmark truck flows against the same period in 2019. Since the 2019 BMI only covers the Chinese new year period, we can only use the change in population flows relative to the same period in 2019 by the lunar calendar. Therefore, our BMI sample only covers the Chinese new year in 2021 and 2022 (before January 31, 2022). The sample covers 8 out of 16 full-scale lockdowns and 10 out of 22 partial lockdowns. We convert daily data ($\mathrm{d}\ln Flow_{ni,t}$) into weekly data by taking the average of $\mathrm{d}\ln Flow_{ni,t}$ in the week. We then apply the same event study approach to the change in city-pair population flows.

Figure A7: Event Study: Weekly City-Pair Population Flows

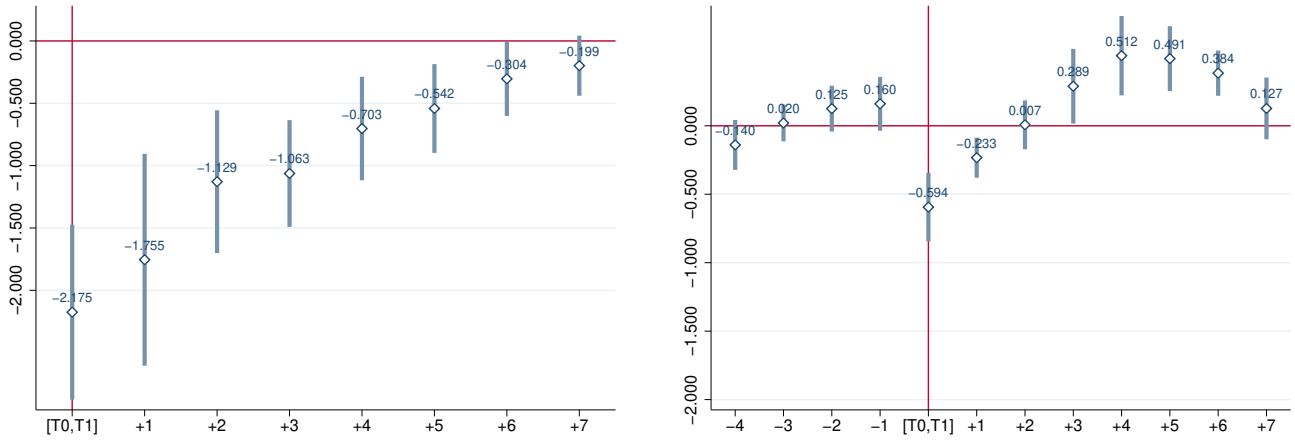

(a) Full-scale lockdown

(b) Partial lockdown

Note: The figure plots the effects of full-scale lockdown (left panel) and partial lockdown (right panel) on $\mathrm{d}\ln Flow_{ni,t}$, together with their 95% confidence intervals.

The estimates are plotted in Figure A7. First note that there are no observations to estimate the pre-trend for full-scale lockdowns. All the six full-scale lockdowns in our BMI sample happened 23 days earlier than the Chinese new year. While we are unable to rule out a pre-trend, we find large effects of a full-scale lockdown on weekly population flows (left panel). On impact, population flows drop by 2.18 log points. The effect gradually diminishes to an insignificant level in six weeks after the end of the lockdown. The partial lockdowns in the BMI

[39] The mean of the two measures differs by 0.3% in 2019.

sample have a wider spread over the Chinese new year period. We find no pre-trend and smaller effects (right panel). Population flows rebound to a higher level in the third week and peak in the fourth week after the lockdown ends. The effect becomes insignificant in the seventh week. Due to data limitations, we cannot examine the dynamics of the lockdown effects in a longer term.

A.7 Estimation of Expenditure Share Matrix

The city-to-city expenditure share matrix is not directly observable. We adopt two approaches to estimate the matrix. The first approach is to apply the gravity model to estimate city-to-city trade flows by China's regional input-output table in 2012, the most recent one published by China's National Bureau of Statistics. Some more recent non-official regional IO tables are also used for robustness check. The second approach is to use city-to-city trade flows in Gao et al. (2020) and Luo (2020), which are directly constructed from China's value-added invoice data.[40] The expenditure shares estimated using the NBS IO table show strong correlation with those derived from CEADS2012 and CEADS2015, with correlation coefficients of 0.973 and 0.996, respectively. The correlation coefficient with estimates based on invoice data is 0.668. The estimated economic impacts are highly correlated across different approaches.

The gravity model assumes that the trade flow between two cities, (X_{ij}), is a function of the total supply of the exporter, (E_j), the total demand of the importer, (M_i), and the impedance of transportation costs, for which the distance between two regions is often used as a proxy (D_{ij}).[41] The standard gravity model is as follows:

$$X_{ij} = G^{\beta_0} \frac{(E_j)^{\beta_1} \times (M_i)^{\beta_2}}{(D_{ij})^{\beta_3}},$$

where G is a constant term. The equation in logarithmic form is:

$$\ln X_{ij} = \beta_0 + \beta_1 \ln E_j + \beta_2 \ln M_i + \beta_3 \ln D_{ij}.$$

Due to limited information on exports and imports at the city level, we make the following assumptions:[42]

$$\ln E_j = \alpha_0 + \alpha_1 \ln GDP_j,$$

$$\ln M_i = \gamma_0 + \gamma_1 \ln GDP_i.$$

[40] See Gao et al. (2020) for a detailed description that connects China's value-added invoice tax data to the regional IO table.

[41] See more discussions about the gravity model in Carrère et al. (2020).

[42] In estimating the expenditure share matrix, we employ a log-linear relationship between cities' trade flows (exports and imports) and their GDP. Our model, instead, focuses on the short-term effects of trade cost shocks.

The gravity model becomes:

$$\ln X_{ij} = \eta_0 + \eta_1 \ln GDP_j + \eta_2 \ln GDP_i + \eta_3 \ln D_{ij},$$

where $\eta_0 = \beta_0 + \beta_1\alpha_0 + \beta_2\gamma_0$, $\eta_1 = \beta_1\alpha_1$, $\eta_2 = \beta_2\gamma_1$ and $\eta_3 = \beta_3$.

We now use the data at the provincial level to estimate the coefficients $\{\eta_0, \eta_1, \eta_2, \eta_3, \alpha_0, \alpha_1, \gamma_0, \gamma_1\}$, which will be used to back out city-to-city trade flows. The province-to-province trade flow data and provincial GDP are from Liu et al. (2018). The distance between two provinces is proxied by the distance between their capital cities. The results of the regressions are reported in Table A4.

Table A4: Regression of Gravity Model

	(1) $\ln X_{pq}$	(2) $\ln E_q$	(3) $\ln M_p$
$\ln GDP_q$	1.0031	1.0692	
	(0.0257)	(0.0243)	
$\ln GDP_p$	0.7256		1.0033
	(0.0188)		(0.0162)
$\ln D_{pq}$	-0.1241		
	(0.0287)		
Constant	-10.5737	0.2891	0.9544
	(0.3895)	(0.2351)	(0.1489)
Observations	917	31	31
R-squared	0.8352	0.9908	0.9911

Note: Robust standard errors are reported in parentheses.

We use the results in Columns (1) and (2) to back out city-to-city trade flow, X_{ij}

$$X_{ij} = \begin{cases} \exp\left(\hat{\eta}_0 + \hat{\eta}_1 \ln GDP_j + \hat{\eta}_2 \ln GDP_i + \hat{\eta}_3 \ln D_{ij}\right) & , \text{ if } i \neq j \\ \exp\left(\hat{\alpha}_0 + \hat{\alpha}_1 \ln GDP_j\right) - \sum_{n \neq j} X_{nj} & , \text{ if } i = j \end{cases}$$

Note that the within-city trade flow of city j is estimated by its total exports minus the sum of its between-city exports.[43] The estimated X_{ij} gives the expenditure share matrix used in the paper.

We then apply the same method to the 2012 and 2015 regional IO tables constructed by Ou et al. (2019) (CEADS2012) and Zheng et al. (2020) (CEADS2015).[44] Last, we also use

[43] One may also use Column (1) and (3) to back out X_{ij} and the expenditure share matrix. The results are similar.

[44] CEADS2012 and CEADS2015 are from https://www.ceads.net/data/input_output_tables/.

the city-to-city trade flows constructed by value-added invoice tax data in 2018 (Luo, 2020) to estimate the economic costs of lockdowns.

A.8 Additional Tables and Figures

Figure A8: Truck Outflow, GDP and Night Light

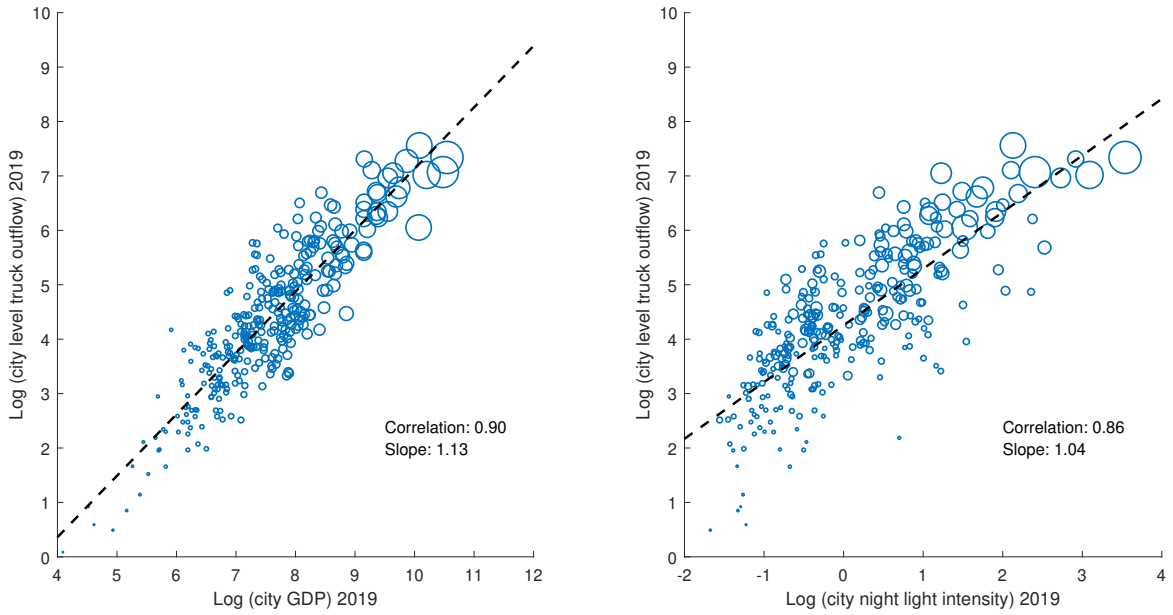

Note: The nightlight data is from the Visible Infrared Imaging Radiometer Suite (VIIRS) Day/Night Band (DNB), which uses average radiance composite images produced by the Earth Observations. These images are produced in 15 arc-second geographic grids. We use the average radiance value of all observations in a city as the city-level nightlight intensity.

Figure A9: Lockdown and City's Size

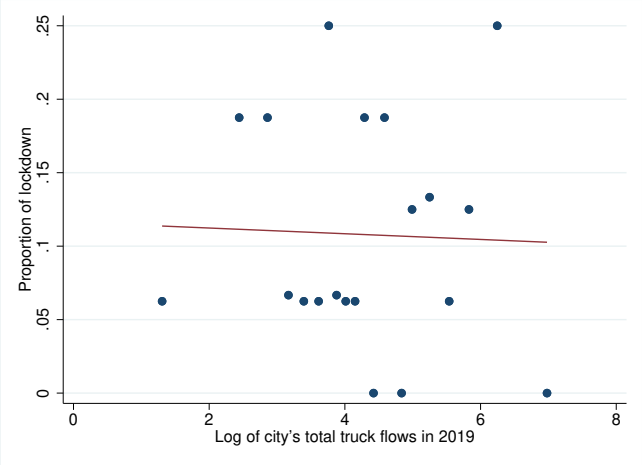

(a) Lockdown and city's truck flows

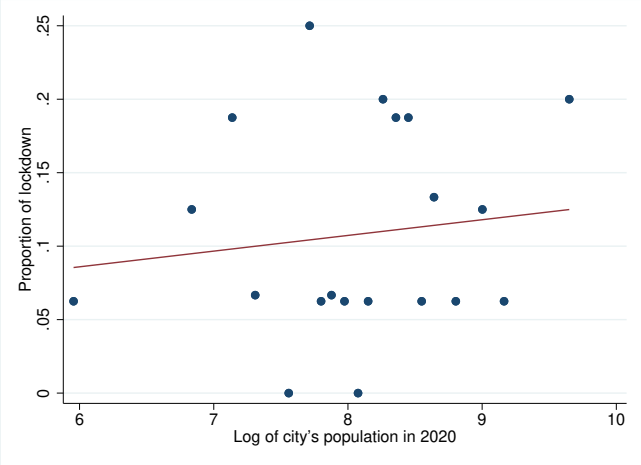

(b) Lockdown and city's population

Note: We sort cities into 20 groups of equal size by the total truck flows connected to the city in 2019 (left panel) or total population of the city in 2020 (right panel). The x-axis is the log truck flow (left panel) or log population (right panel). The y-axis is the proportion of the cities that experienced lockdown in each group. The slope of the fitted line (solid line) is statistically insignificant in both panels.

Figure A10: Event Study with Two-way Clustering

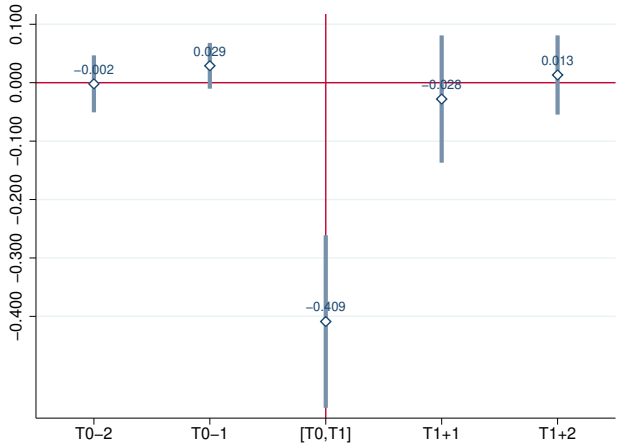

(a) Full-scale lockdown

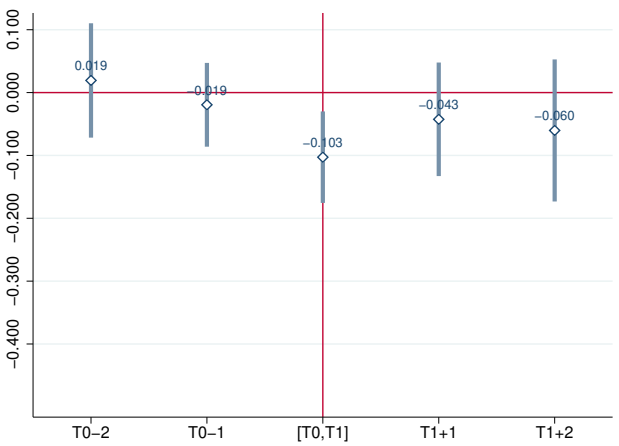

(b) Partial lockdown

Note: The figure reproduces Figure 2, with the standard errors clustered at both cities in the city pair (Cameron et al., 2011).

Table A5: Effects of Lockdown on Real Income, Robustness Check

		Benchmark	$\theta = 2$	$\theta = 6$	CEADS2012	CEADS2015	INVOICE
Shijiazhuang	Real income change of lockdown cities	-60.45%	-59.43%	-60.72%	-61.47%	-59.38%	-57.70%
	Real national income change	-0.40%	-0.41%	-0.39%	-0.41%	-0.39%	-0.40%
	Spillover effects	8.57%	13.60%	6.45%	9.73%	7.94%	13.33%
Big 4 cities	Real income change of lockdown cities	-61.85%	-60.74%	-62.16%	-63.06%	-59.78%	-56.01%
	Real national income change	-8.69%	-8.92%	-8.58%	-8.92%	-8.34%	-9.05%
	Spillover effects	8.54%	12.51%	6.92%	9.22%	7.98%	20.47%
All cities	Real national income change	-51.82%	-51.79%	-51.71%	-50.27%	-51.83%	-46.62%

Note: The first column reports the benchmark counterfactual results. The second and third columns report the results in the model with $\theta = 2$ and $\theta = 6$, respectively. The last three columns maintain the benchmark value of θ but use different expenditure share matrices implied by the city-level IO tables in Appendix A.7. "Big 4 cities" refers to Beijing, Shanghai, Guangzhou, and Shenzhen. The effects of full-scale lockdown in all the robustness checks are obtained by conducting the counterfactual exercises in the models with re-estimated lockdown effects on the between- and within-city composite costs under different values of θ or expenditure share matrix.

A.9 Proof of Proposition 1

The consumer in city n needs to solve the following utility maximization problem

$$\max_{\{Q_{ni}\}} \boldsymbol{u}_n = \left(\sum_{i=1}^{N} Q_{ni}^{\frac{\theta}{\theta+1}} \right)^{\frac{\theta+1}{\theta}}$$

subject to

$$\sum_{i=1}^{N} (\tau_{ni} w_i / a_i) Q_{ni} = e_n,$$

where Q_{ni} is the trade flows of goods i consumed in city n in quantity; $\theta + 1$ is the elasticity of substitution across goods; $\tau_{ni} w_i / a_i$ is the price of goods i to city n; and $e_n \equiv w_n \ell_n + \bar{d}_n$ is the nominal total expenditure of city n. The first-order conditions of the above problem are

$$\frac{Q_{ni}}{Q_{nk}} = \left(\frac{\tau_{ni} w_i / a_i}{\tau_{nk} w_k / a_k} \right)^{-(1+\theta)}, \quad \forall i, k = 1, ..., N. \tag{29}$$

Equation (29) directly gives the expression of the equilibrium expenditure share S_{ni} as in the second part of equation (6).

Let $\boldsymbol{e}$ be the vector of nominal expenditure and $\boldsymbol{\pi}$ be the vector of nominal income ($\pi_n \equiv w_n \ell_n$). We also define

$$T_{ni} \equiv S_{in} e_i / \pi_n$$

as the income share of city n derived from market i.

Then we have

$$\boldsymbol{\pi}' = \boldsymbol{e}'\boldsymbol{S} \tag{30}$$

$$\boldsymbol{e}' = \boldsymbol{\pi}'\boldsymbol{T} \tag{31}$$

Let $\boldsymbol{d}$ as the vector of city n's income-to-expenditure ratio ($d_n \equiv \pi_n/e_n$), which is equal to 1 with balanced trade. Let $\boldsymbol{D} \equiv Diag(\boldsymbol{d})$ be the diagonalization of the vector $\boldsymbol{d}$.

We define the average changes in outgoing costs from city i as

$$\mathrm{d}\ln Z_i^{out} = \sum_n T_{in}\,\mathrm{d}\ln z_{ni},$$

and the average changes in incoming costs to city i as

$$\mathrm{d}\ln Z_i^{in} = \sum_n S_{in}\,\mathrm{d}\ln z_{in}.$$

Taking total differentiation of equations (4), (6) and (7) and putting them together, we have

$$(\theta+1)\,\mathrm{d}\ln\pi_n = \theta\left(\sum_i T_{ni}\,\mathrm{d}\ln Z_i^{in} - \mathrm{d}\ln Z_n^{out}\right) + \theta\sum_{i,k} T_{ni}S_{ik}\,\mathrm{d}\ln\pi_k + \sum_i T_{ni}\,\mathrm{d}\ln e_i,$$

or in matrix

$$\mathrm{d}\ln\boldsymbol{\pi} = [(\theta+1)\mathbf{1} - \theta\boldsymbol{T}\boldsymbol{S} - \boldsymbol{T}\boldsymbol{D} + \mathbf{1}\boldsymbol{\pi}']^{-1}\,\theta(\boldsymbol{T}\,\mathrm{d}\ln\boldsymbol{Z}^{in} - \mathrm{d}\ln\boldsymbol{Z}^{out}) \tag{32}$$

Again from equation (6) we have

$$\begin{aligned}\mathrm{d}\ln Q_{ni} &= \mathrm{d}\ln S_{ni} + \mathrm{d}\ln e_n - \mathrm{d}\ln\pi_i - \mathrm{d}\ln z_{ni} \\ &= -(\theta+1)\,(\,\mathrm{d}\ln z_{ni} + \mathrm{d}\ln\pi_i) + \theta\,\mathrm{d}\ln Z_n^{in} + \theta\sum_k S_{nk}\,\mathrm{d}\ln\pi_k + \mathrm{d}\ln e_n,\end{aligned}$$

and in matrix

$$\mathrm{d}\ln\boldsymbol{Q} = -(\theta+1)\,(\,\mathrm{d}\ln\boldsymbol{Z} + \mathbf{1}\,\mathrm{d}\ln\boldsymbol{\pi}') + \theta\,\mathrm{d}\ln\boldsymbol{Z}^{in}\mathbf{1}' + (\theta\boldsymbol{S} + \boldsymbol{D})\,\mathrm{d}\ln\boldsymbol{\pi}\mathbf{1}' \tag{33}$$

Now we stack the matrixes $\mathrm{d}\ln \boldsymbol{Z}$ and $\mathrm{d}\ln \boldsymbol{Q}$ into vectors $\mathrm{d}\ln \boldsymbol{\mathcal{Z}}$ and $\mathrm{d}\ln \boldsymbol{\mathcal{Q}}$, respectively:

$$\mathrm{d}\ln \boldsymbol{\mathcal{Z}} \equiv \begin{bmatrix} \mathrm{d}\ln z_{11} \\ \vdots \\ \mathrm{d}\ln z_{1N} \\ \vdots \\ \mathrm{d}\ln z_{N1} \\ \vdots \\ \mathrm{d}\ln z_{NN} \end{bmatrix}_{N^2\times 1} \qquad \mathrm{d}\ln \boldsymbol{\mathcal{Q}} \equiv \begin{bmatrix} \mathrm{d}\ln Q_{11} \\ \vdots \\ \mathrm{d}\ln Q_{1N} \\ \vdots \\ \mathrm{d}\ln Q_{N1} \\ \vdots \\ \mathrm{d}\ln Q_{NN} \end{bmatrix}_{N^2\times 1}$$

Equation (32) can be simplified as

$$\mathrm{d}\ln \boldsymbol{\pi} = \theta \boldsymbol{V} \left(\boldsymbol{T}\tilde{\boldsymbol{S}} - \tilde{\boldsymbol{T}} \right) \mathrm{d}\ln \boldsymbol{\mathcal{Z}}, \tag{34}$$

where $\boldsymbol{V} = [(\theta+1)\boldsymbol{I} - \theta \boldsymbol{T}\boldsymbol{S} - \boldsymbol{T}\boldsymbol{D} + \boldsymbol{1}\boldsymbol{\pi}']^{-1}$ and

$$\tilde{\boldsymbol{S}} = \begin{bmatrix} \boldsymbol{S}_1 & & \\ & \ddots & \\ & & \boldsymbol{S}_N \end{bmatrix}_{N\times N^2} \quad \text{with} \quad \boldsymbol{S}_n = \begin{bmatrix} S_{n1} & \cdots & S_{nN} \end{bmatrix}_{1\times N},$$

$$\tilde{\boldsymbol{T}} = \begin{bmatrix} \boldsymbol{T}_1 & \cdots & \boldsymbol{T}_N \end{bmatrix}_{N\times N^2} \quad \text{with} \quad \boldsymbol{T}_n = \begin{bmatrix} T_{1n} & & \\ & \ddots & \\ & & T_{Nn} \end{bmatrix}_{N\times N}.$$

Together with equations (33) and (34), we have

$$\mathrm{d}\ln \boldsymbol{\mathcal{Q}} = \boldsymbol{G}\, \mathrm{d}\ln \boldsymbol{\mathcal{Z}} \tag{35}$$

where $\boldsymbol{G} = -(\theta+1)\boldsymbol{\mathcal{I}} + \left[-(\theta+1)\boldsymbol{\mathcal{I}}^{out} + \boldsymbol{\mathcal{I}}^{in}(\theta \boldsymbol{S} + \boldsymbol{D})\right] \theta \boldsymbol{V} \left(\boldsymbol{T}\tilde{\boldsymbol{S}} - \tilde{\boldsymbol{T}} \right) + \theta \boldsymbol{\mathcal{I}}^{in} \tilde{\boldsymbol{S}}$ is an $N^2 \times N^2$ matrix; $\boldsymbol{\mathcal{I}}$ is an $N^2 \times N^2$ identity matrix; $\boldsymbol{I}$ is an $N \times N$ identity matrix; $\boldsymbol{1}$ is an $N \times 1$ vector with all the entries equal to one; and

$$\boldsymbol{\mathcal{I}}^{out} = \begin{bmatrix} \boldsymbol{I} \\ \vdots \\ \boldsymbol{I} \end{bmatrix}_{N^2\times N} \qquad \boldsymbol{\mathcal{I}}^{in} = \begin{bmatrix} \boldsymbol{1} & & \\ & \ddots & \\ & & \boldsymbol{1} \end{bmatrix}_{N^2\times N}$$

This proves the first part of Proposition 1.

Next, total differentiation on equation (5) gives us

$$\mathrm{d}\ln \boldsymbol{u}_n = \sum_{i=1}^{N} \frac{Q_{ni}^{\theta/(\theta+1)}}{\sum_{k=1}^{N} Q_{nk}^{\theta/(\theta+1)}} \mathrm{d}\ln Q_{ni}. \tag{36}$$

With equations (6) and (29), we have

$$\frac{Q_{ni}^{\theta/(\theta+1)}}{\sum_{k=1}^{N} Q_{nk}^{\theta/(\theta+1)}} = \frac{(\tau_{ni} w_i / z_i)^{-\theta}}{\sum_{k=1}^{N} (\tau_{nk} w_k / z_k)^{-\theta}} = S_{ni}. \tag{37}$$

Taking equation (37) into equation (36), we have

$$\mathrm{d}\ln \boldsymbol{u}_n = \sum_{i=1}^{N} S_{ni} \mathrm{d}\ln Q_{ni},$$

which proves the second part of Proposition 1.

A.10 Closed-form Solution of Structural Approaches

To obtain analytical expressions for closed-form solution in structural approaches, we introduce the following notations:

$$\mathrm{d}\ln \boldsymbol{\mathcal{Q}}_t \equiv \begin{bmatrix} \mathrm{d}\ln Q_{11,t} \\ \vdots \\ \mathrm{d}\ln Q_{1N,t} \\ \vdots \\ \mathrm{d}\ln Q_{N1,t} \\ \vdots \\ \mathrm{d}\ln Q_{NN,t} \end{bmatrix}_{N^2\times 1}, \quad \boldsymbol{\mathcal{D}}_t^k \equiv \begin{bmatrix} D_{11,t}^k \\ \vdots \\ D_{1N,t}^k \\ \vdots \\ D_{N1,t}^k \\ \vdots \\ D_{NN,t}^k \end{bmatrix}_{N^2\times 1}, \quad \boldsymbol{\mathcal{W}}_t \equiv \begin{bmatrix} W_{11} \\ \vdots \\ W_{1N} \\ \vdots \\ W_{N1} \\ \vdots \\ W_{NN} \end{bmatrix}_{N^2\times 1}$$

for $k = h, l$ and $t = 1, 2, \cdots, T$. Also let

$$\boldsymbol{I}(n=i) \equiv \begin{bmatrix} 1 & & & & \\ & \ddots & & & \\ & & \mathbf{1}(n=i) & & \\ & & & \ddots & \\ & & & & 1 \end{bmatrix}_{N^2\times N^2}, \quad \boldsymbol{I}(n\neq i) \equiv \begin{bmatrix} 0 & & & & \\ & \ddots & & & \\ & & \mathbf{1}(n\neq i) & & \\ & & & \ddots & \\ & & & & 0 \end{bmatrix}_{N^2\times N^2}$$

By Proposition 1, the simulated trade flow quantity changes can be written as

$$\mathrm{d}\ln \hat{\boldsymbol{\mathcal{Q}}}_t = \boldsymbol{G}\left[\boldsymbol{I}(n \neq i)\boldsymbol{\mathcal{D}}_t \quad \boldsymbol{I}(n = i)\boldsymbol{\mathcal{D}}_t\right]\Psi, \tag{38}$$

where

$$\boldsymbol{\mathcal{D}}_t = \left[\boldsymbol{\mathcal{D}}_t^h \quad \boldsymbol{\mathcal{D}}_t^l\right], \quad \Psi = \begin{bmatrix} \beta^h \\ \beta^l \\ \gamma^h \\ \gamma^l \end{bmatrix} \tag{39}$$

Last, let

$$\boldsymbol{X} = \begin{bmatrix} \boldsymbol{G}\boldsymbol{I}(n \neq i)\boldsymbol{\mathcal{D}}_1 & \boldsymbol{G}\boldsymbol{I}(n = i)\boldsymbol{\mathcal{D}}_1 \\ \vdots & \vdots \\ \vdots & \vdots \\ \boldsymbol{G}\boldsymbol{I}(n \neq i)\boldsymbol{\mathcal{D}}_T & \boldsymbol{G}\boldsymbol{I}(n = i)\boldsymbol{\mathcal{D}}_T \end{bmatrix}, \boldsymbol{Y} = \begin{bmatrix} \mathrm{d}\ln \boldsymbol{\mathcal{Q}}_1 \\ \vdots \\ \vdots \\ \mathrm{d}\ln \boldsymbol{\mathcal{Q}}_T \end{bmatrix}, \boldsymbol{W} = \begin{bmatrix} \boldsymbol{\mathcal{W}}_1 \\ \vdots \\ \vdots \\ \boldsymbol{\mathcal{W}}_T \end{bmatrix},$$

where T denotes the total number of periods in our sample.

The close-formed solution to the estimation of Ψ in (10) is given by

$$\hat{\Psi} = \left(\boldsymbol{X}'\boldsymbol{W}\boldsymbol{X}\right)^{-1}\boldsymbol{X}'W\boldsymbol{Y}.$$